

Dalton Transactions

Accepted Manuscript



This is an *Accepted Manuscript*, which has been through the Royal Society of Chemistry peer review process and has been accepted for publication.

Accepted Manuscripts are published online shortly after acceptance, before technical editing, formatting and proof reading. Using this free service, authors can make their results available to the community, in citable form, before we publish the edited article. We will replace this *Accepted Manuscript* with the edited and formatted *Advance Article* as soon as it is available.

You can find more information about *Accepted Manuscripts* in the [Information for Authors](#).

Please note that technical editing may introduce minor changes to the text and/or graphics, which may alter content. The journal's standard [Terms & Conditions](#) and the [Ethical guidelines](#) still apply. In no event shall the Royal Society of Chemistry be held responsible for any errors or omissions in this *Accepted Manuscript* or any consequences arising from the use of any information it contains.

The Important Role of the Anion Coligands in Promoting Structural and Magnetic Diversity in unusual mixed-bridged Polynuclear Ni^{II} Complexes with a versatile bis(2-methoxy phenol)diamine hexadentate ligand. An Experimental and Theoretical Magneto-Structural Study

L. Botana,^b José Ruiz,^a Antonio J. Mota,^a Antonio Rodríguez-Diéguez,^a José M. Seco,^{*,b} Itziar Oyarzabal,^b Enrique Colacio^{*,a}

a) Departamento de Química Inorgánica, Facultad de Ciencias, Universidad de Granada, Av. Fuentenueva S/N, 18071 Granada (Spain). Email: ecolacio@ugr.es.

b) Departamento de Química Aplicada, Facultad de Química, UPV/EHU, Paseo Manuel Lardizabal, n° 3, 20018, Donostia-San Sebastián, Spain.

Abstract

This work reports the syntheses, crystal structures, magnetic properties and DFT calculations of six novel polynuclear Ni^{II} compounds [Ni₂(μ-HL¹)₂(μ-N₃)]N₃·(CH₃OH)₂·2H₂O (**1**), [Ni₂(μ-HL¹)₂(μ-N₃)]Na₂Ni₂(μ-L¹)₂(μ-N₃)₂(CH₃OH)(N₃)·4CH₃OH (**2**), [Ni₄(μ-L¹)₂(μ-N₃)₄(CH₃OH)₂]·2CH₃OH (**3**), [Na₂Ni₄(μ-L¹)₂(μ-OAc)₂(μ-N₃)₄(CH₃OH)₄]·2CH₃OH (**4**), [Ni₄(μ-L¹)₂(μ-Cl)₂(Cl)₂] (**5**), [Ni₃(μ-L¹)₂(acac)₂(H₂O)₂] (**6**), with uncommon structures and rare mixed-bridges between Ni^{II} ions, which were prepared from the versatile polytopic Mannich base ligand *N,N*-dimethyl-*N,N'*-bis(2-hydroxy-3-methoxy-5-methylbenzyl)ethylenediamine (H₂L¹). The anionic coligand (azide, chloride, acetate and acetylacetonate) and reaction conditions play a crucial role in determining the final structure of these compounds and consequently in their magnetic properties. Compound **1** contains a Ni₂ cationic unit with rare di-μ-phenoxido/μ_{1,1}-azide triple mixed bridges whereas complex **2** is made from the same Ni₂ cationic unit as in **1**, cocrystallized with Na₂Ni₂ neutral units, in which double μ_{1,1}-azide bridges connect the Ni^{II} ions, and azide anions. Complexes **3** and **4** are Ni₄ complexes with linear and defective dicubane structures, respectively. In **3**, rare μ-phenoxido/μ_{1,1}-azide/syn-syn acetate triple mixed bridges connect central and terminal Ni^{II} atoms whereas a double μ_{1,1,1}-azide planar bridging fragment links the central Ni^{II} ions. Complex **4**, has two distinct types of mixed bridges, μ-phenoxido/μ_{1,1,1}-azido and μ_{1,1}-azido/μ_{1,1,1}-azido and a double di-μ_{1,1,1}-azido bridge, the latter connecting the face-sharing Ni^{II} ions. Complex **5** has a defective-dicubane structure with double μ-phenoxido/μ₃-chloro mixed bridges and di-μ₃-chloro bridges, whereas complex **6** has a bent structure with very uncommon single μ-phenoxido bridges. The analysis of the

2014/07/15

magnetic properties reveals that in complexes **1-4** all magnetic pathways transmit ferromagnetic interactions leading to $S = 2$ ground states for **1** and **2** and $S = 4$ ground states for **3** and **4**. In complex **5**, the double μ -phenoxido/ μ_3 -chloro mixed bridges and di- μ_3 -chloro bridges mediate antiferro- and ferromagnetic interactions, respectively, giving rise to a $S = 0$ ground state. Complex **6** shows antiferromagnetic interactions between the Ni^{II} ions through single μ -phenoxido bridging groups, leading to an $S = 1$ ground state. DFT calculations on the X-ray structures and model compounds were performed to support the magneto-structural data of the above compounds.

Introduction

Polynuclear transition metal complexes with unpaired electrons in the spin ground state have been profusely studied during the last few decades because of their relevance, among other fields, in metalloenzymes¹ and molecular magnetism.² With regard to the latter field, special attention has been recently focused in the search for coordination clusters exhibiting slow relaxation of the magnetization and magnetic hysteresis below the so-called blocking temperature, T_B . These intriguing nanomagnets, called Single-Molecule Magnets (SMMs),³ have been suggested for applications in molecular spintronics, ultra-high density magnetic information storage and quantum computing at molecular level.⁴ The SMM behaviour is the result of a large spin ground state that undergoes considerable Ising-type axial magnetic anisotropy (D), which gives rise to an energy barrier (U) that prevents reversal of the molecular magnetization when the field is removed, leading to bistability.^{1a} The spin multiplicity of the ground state in homo- and heteronuclear coordination clusters mainly depends on the nature of the metal ions, the magnetic exchange interactions between them and their topology.⁵ Therefore, to design systems with high spin ground states it is very helpful to understand which are the main structural factors governing the magnetic exchange interactions through the bridging ligands. In this regard, the experimental and theoretical magneto-structural correlations, most of them derived from studies on dinuclear complexes, are very useful tools for qualitatively assessing the magnetic coupling in coordination clusters and then to get molecule-based materials with predicted magnetic properties. Therefore, the adequate choice of the ligand (with specific donor sites and bridging modes), metal ions (with specific spin and preferred stereochemistry) and anionic coligands (either with an ancillary or bridging function) play a crucial role in determining the final

architecture of the polynuclear complex and consequently its ground state and magnetic properties.

We have recently shown that the Mannich base hexadentate ligand *N,N'*-dimethyl-*N,N'*-bis(2-hydroxy-3-methoxy-5-methylbenzyl)ethylenediamine (H_2L^1) is able to form bis(μ -diphenoxido) Cu_3 complexes, where the ligand acts in a compartmental form (see Scheme 1, coordination mode a), with the two deprotonated phenol groups bridging copper(II) ions, and the methoxy groups remain uncoordinated.⁶ The coordination chemistry of the H_2L^1 ligand remains almost unexplored and, to the best of our best of our knowledge, only one additional paper dealing $CuLn$ ($Ln^{3+} = Gd, Tb, Dy$) complexes has been very recently published, where the ligand acts in a compartmental mode but with the methoxy groups coordinated to the Ln^{3+} ion (see scheme 1, coordination mode b).⁷ As the H_2L^1 ligand is more flexible than the Schiff base counterparts, it should exhibit a higher versatility also allowing the adoption of an open form with new coordination modes (see Scheme 1). Therefore, the assembly of the fully- and semi-deprotonated ligand with metal ions and other anionic coligands (which can also act as bridging ligands), would be a good strategy to obtain polynuclear complexes exhibiting a wide diversity of structural types and magnetic properties.

Following this strategy, in this paper we report on the synthesis, structural characterization, magnetic properties and DFT theoretical calculations of six new polynuclear Ni^{II} complexes with different anionic coligands (azide, chloride and acetylacetonate) where the fully or semideprotonated H_2L^1 ligand acts in a open form with different coordination modes. The Ni^{II} ion has been chosen because it has considerable magnetic anisotropy generated from the second order spin-orbit coupling and therefore it is a promising candidate for preparing SMMs (despite this, only a few examples of nickel(II) single-molecule magnets have been reported so far).⁸ It should be noted that the combination of a diphenoxido-bridged Ni^{II} fragment with other bridging ligands may lead to uncommon mixed-bridged fragments able to mediate ferromagnetic interactions between the metal ions, thus favouring a high spin ground state of the complex.

When azide is used as coligand three different phenoxide/azide mixed-bridged complexes are obtained: a dinuclear complex $[Ni_2(\mu-HL^1)_2(\mu-N_3)]N_3 \cdot (CH_3OH)_2 \cdot 2H_2O$ (**1**) with a rare triple diphenoxido($\mu_{1,1,1}-N_3$) bridge connecting the Ni^{II} ions, a complex salt $[Ni_2(\mu-HL^1)_2(\mu-N_3)][Na_2Ni_2(\mu-L^1)_2(\mu-N_3)_2(CH_3OH)(N_3)] \cdot 4CH_3OH$ (**2**), where the cation is the dinuclear entity of compound **1** and the anion a defective dicubane Ni_2Na_2 anionic

2014/07/15

tetranuclear complex unit with double $\mu_{1,1,1}$ -N₃ bridges connecting the Ni^{II} ions and phenoxide/ $\mu_{1,1,1}$ -N₃ bridges linking the Ni^{II} and Na ions, and, finally, a defective dicubane Ni₄ tetranuclear complex [Ni₄(μ -L¹)₂(μ -N₃)₄(CH₃OH)₂] \cdot 2CH₃OH (**3**) containing uncommon $\mu_{1,1,1}$ -N₃/ $\mu_{1,1,1}$ -N₃ and phenoxido/ $\mu_{1,1,1}$ -N₃ bridges connecting the Ni^{II} ions. A combination of azide and acetate leads to the zig-zag hexanuclear complex [Na₂Ni₄(μ -L¹)₂(μ -OAc)₂(μ -N₃)₄(CH₃OH)₄] \cdot 2CH₃OH (**4**), with one double $\mu_{1,1,1}$ -N₃ and two triple phenoxido/acetate/ $\mu_{1,1,1}$ -N₃ triple bridge connecting the Ni^{II} ions. With chloride as coligand, the defective dicubane Ni₄ tetranuclear complex [Ni₄(μ -L¹)₂(μ -Cl)₂(Cl)₂] (**5**) was obtained, where the Ni^{II} ions are linked by double μ_3 -Cl and phenoxide/ μ_3 -Cl bridges. Finally, using Ni(acac)₂ as source of Ni^{II} the single-phenoxido bridged bent trinuclear Ni₃ complex [Ni₃(μ -L¹)₂(acac)₂(H₂O)₂] (**6**) could be obtained. Complexes **1-4** and **5-6** exhibit overall ferromagnetic and antiferromagnetic interactions, respectively.

Experimental

Materials and Physical Measurements. All reagents were obtained from commercial sources and used as received. N,N'-dimethyl-N,N'-bis(2-hydroxy-3-methoxy-5-methylbenzyl)ethylenediamine, H₂L¹ (Scheme I) was prepared following a reported procedure.⁹ Elemental (C, H, and N) analyses were performed on a Leco CHNS-932 microanalyzer. IR spectra were recorded in the region 400-4000 cm⁻¹ on a Nicolet 6700 FTIR spectrophotometer with samples as KBr disks. Variable-temperature magnetic susceptibility and magnetization measurements were carried out with a magnetometer Quantum Design SQUID MPMS XL5 for **1,2** and **6**, SQUID MPMS-7T for **3** and Model 6000 PPMS for **4** and **5**. Diamagnetic corrections were estimated from the Pascal's constants.

Computational Details.

All theoretical calculations were carried out at the density functional theory (DFT) level using the hybrid B3LYP exchange-correlation functional,¹⁰ as implemented in the Gaussian 09 program.¹¹ A quadratic convergence method was employed in the self-consistent-field process.¹² The triple- ζ quality basis set proposed by Ahlrichs and co-workers has been used for all atoms.¹³ Calculations were performed on complexes built from

experimental geometries as well as on model complexes. The electronic configurations used as starting points were created using Jaguar 7.9 software.¹⁴ The approach used to determine the exchange coupling constants for polynuclear complexes has been described in detail elsewhere.¹⁵

Crystallographic Refinement and Structure Solution.

Single crystals of suitable dimensions were used for data collection. For compounds **1**, **2**, **3** and **6** diffraction intensities were collected on a Bruker SMART APEX CCD diffractometer, with graphite-monochromated Mo K α ($\lambda = 0.71073 \text{ \AA}$) radiation at 100 K. For data reduction, the “Bruker Saint Plus” program was used. The data were corrected for Lorentz and polarization effects, and an empirical absorption correction (SADABS) was applied. Structures were solved by SIR-97 and refined by fullmatrix least-squares methods based on F^2 using SHELXL-97, incorporated in WinGX 1.64 crystallographic collective package.

Intensity data for compounds **4** and **5** were collected at 100 K on a Agilent Technologies SuperNova diffractometer (mirror-monochromated Mo K α radiation, $\lambda = 0.71073 \text{ \AA}$) equipped with Eos CCD detector.

Data collections, unit cell determinations, intensity data integrations, routine corrections for Lorentz and polarization effects and analytical absorption corrections with face indexing were performed using the CrysAlis Pro software package.¹⁶ The structures were solved using OLEX¹⁷ and refined by full-matrix least-squares with SHELXL-97.¹⁸ Final geometrical calculations were carried out with PLATON¹⁹ as integrated in WinGX.²⁰ CCDC reference numbers for the structures of **1-6** are 981150-981155. Refinement special details are given in ESI file.

Crystallographic parameters are summarised in Table S1.

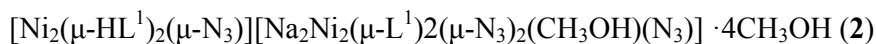
Syntheses of Complexes.

$[\text{Ni}_2(\mu\text{-HL}^1)_2(\mu\text{-N}_3)]\text{N}_3 \cdot (\text{CH}_3\text{OH})_2 \cdot 2\text{H}_2\text{O}$ (**1**).

To a suspension of H_2L^1 (0.048 g, 0.125 mmol) in H_2O (5 mL) a solution of $\text{Ni}(\text{NO}_3)_2 \cdot 4\text{H}_2\text{O}$ (0.036 g, 0.125 mmol) in MeOH (5 mL) was added. The mixture was stirred during 5 minutes until solution and then NaN_3 (0.0825 g, 1.25 mmol) in 1:1

2014/07/15

MeOH/H₂O (10 mL) was added and the mixture additionally stirred for 10 minutes. After one hour, a green solid formed, which was filtered off and the filtrate left undisturbed at room temperature. X-ray-quality green crystals were formed from the filtrate after two days, which were collected by filtration, washed with MeOH/H₂O and dried in vacuum. Yield: 0.0458 g, 68%. Anal. Calcd for C₄₆H₇₄N₁₀O₁₂Ni₂: C, 51.32; H, 6.93; N, 13.01. Found: C, 51.12; H, 7.08; N, 12.94. Selected FT-IR data (cm⁻¹): ν(azide) 2090vs, ν(azide) 2021vs.



The synthesis of this compound is similar to that of **1** but using only methanol (20 mL) as solvent. Yield: 0.033 g, 48%. Anal. Calcd for C₉₄H₁₄₆N₂₀O₂₂Na₂Ni₄: C, 51.58; H, 6.72; N, 12.80. Found: C, 51.47; H, 6.98; N, 13.06. Selected FT-IR data (cm⁻¹): ν(azide) 2093vs, ν(azide) 2049vs.

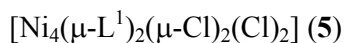


To a solution of NiCl₂·6H₂O (0.118 g, 0.5 mmol) and H₂L¹ (0.096 g, 0.25 mmol) in CH₃OH (10 mL) was added NaN₃ (0.165 g, 2.5 mmol) in CH₃OH (10 mL). The mixture was stirred during 30 minutes, and then was filtered and the filtrate kept undisturbed at room temperature. After two days, crystals of **2** were obtained which were filtered off. The filtrate kept undisturbed at room temperature for two months afforded green X-ray quality crystals of **3**. Yield: 0.036 g, 22%. Anal. Calcd for C₄₈H₇₆N₁₆O₁₂Ni₄: C, 44.21; H, 5.87; N, 17.18. Found: C, 44.06; H, 5.89; N, 17.56. Selected FT-IR data (cm⁻¹): ν(azide) 2073vs.

This compound can also be directly prepared by using the same stoichiometry of the reactants and triethylamine (H₂L¹ /triethylamine = 1:2) to fully deprotonate the ligand.



H₂L¹ (0.048 g, 0.125 mmol) and NaN₃ (0.016 g, 0.25 mmol) were successively added to a solution of Ni(OAc)₂·4H₂O (0.062 g, 0.25 mmol) in MeOH (20 mL). The mixture was stirred during 30 minutes and then was filtered. The filtrate was allowed to stand at room temperature for several days, whereupon green X-ray quality crystals of **4** formed, which were collected by filtration, washed with MeOH/H₂O and dried in vacuum. Yield: 0.042 g, 44%. Anal. Calcd for C₅₄H₉₀N₁₆O₁₈Ni₄Na₂: C, 42.33; H, 5.92; N, 14.63. Found: C, 42.22; H, 5.82; N, 14.83. Selected FT-IR data (cm⁻¹): ν(azide) 2080vs, ν_{as}(COO) 1576vs.



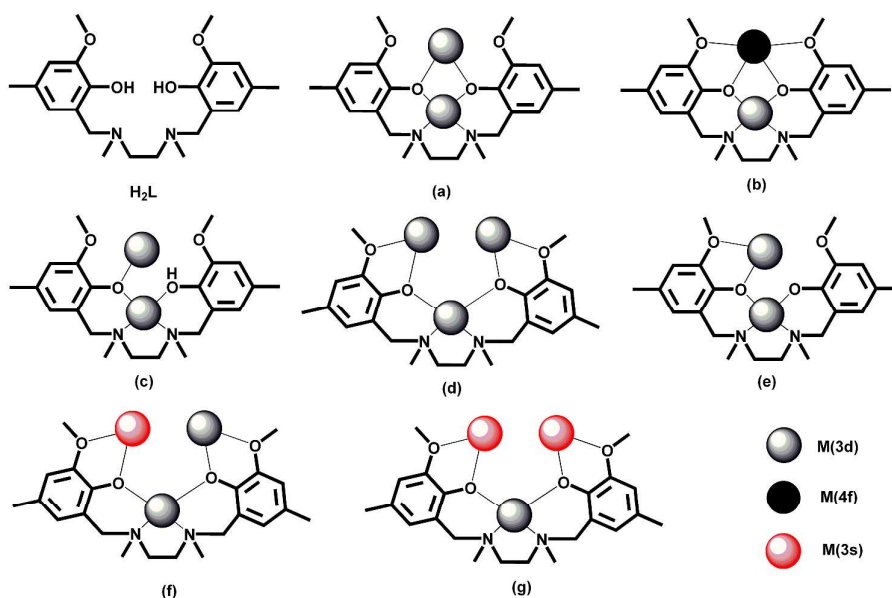
A suspension of $\text{NiCl}_2 \cdot 6\text{H}_2\text{O}$ (0.059 g, 0.25 mmol) and H_2L^1 (0.048 g, 0.125 mmol) in CH_3CN (20 mL) was stirred and warmed up until boiling and then was cooled to room temperature and filtered. The resulting blue solution kept at room temperature for one day afforded red X-ray-quality crystals. Yield: 0.042 g, 58%. Anal. Calcd for $\text{C}_{44}\text{H}_{60}\text{N}_4\text{O}_8\text{Cl}_4\text{Ni}_4$: C, 45.97; H, 5.26; N, 4.87. Found: C, 44.71; H, 5.6; N, 4.68.



To a suspension of H_2L^1 (0.048 g, 0.125 mmol) in acetonitrile (10 mL) was added a suspension of $\text{Ni}(\text{acac})_2$ (0.032 g, 0.125 mmol) in acetonitrile (10 mL). The mixture was stirred during 20 minutes and then was filtered. The filtrate was allowed to stand at room temperature for several days, whereupon X-ray-quality green crystals of **6** were obtained. Yield: 0.031 g, 63%. Anal. Calcd for $\text{C}_{54}\text{H}_{78}\text{N}_4\text{O}_{14}\text{Ni}_3$: C, 54.81; H, 6.64; N, 4.73. Found: C, 54.63; H, 6.92; N, 4.79. Selected FT-IR data (cm^{-1}): $\nu(\text{acac})$ 1606vs.

Results and discussion

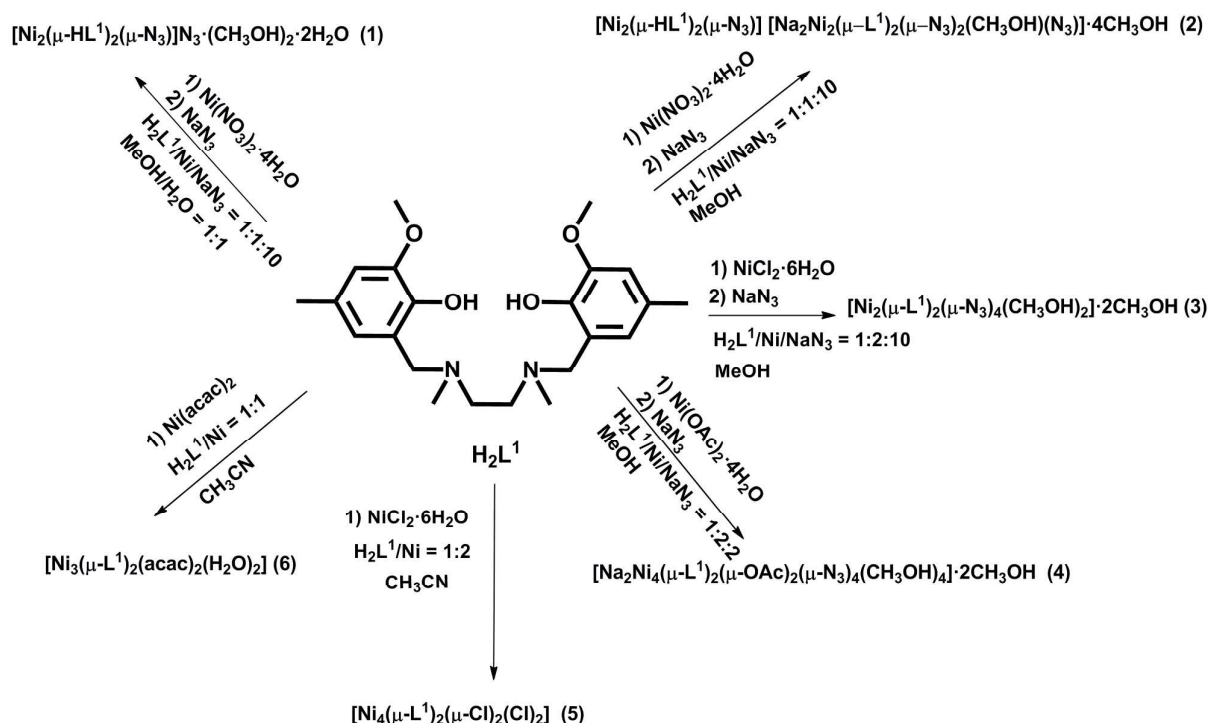
The hexadentate H_2L^1 ligand has been synthesized by using a Mannich type reaction and can exhibit the coordination modes indicated in Scheme 1.



Scheme 1. Structure of H_2L^1 and its coordination modes

The reaction of the H_2L^1 ligand with $\text{Ni}(\text{NO}_3)_2 \cdot 4\text{H}_2\text{O}$ and NaN_3 in a 1:1:10 molar ratio using a methanol/water 1:1 mixture afforded the diphenoxido-azide bridged dinuclear cationic complex **1** (see Scheme 2), in which the monodeprotonated ligand acts in the coordination mode c (Scheme 1).

2014/07/15



Scheme 2. Reactivity of the H₂L¹ ligand and complexes prepared in this work.

Under the same reaction conditions but using only methanol as solvent, the complex **2** was obtained, which is made from the same dinuclear cation complex as **1**, a neutral tetranuclear Na₂Ni₂ complex and one azide as counteranion, where the fully deprotonated ligand exhibits the coordination mode f. The isolation of **2** from the methanol solution may be related with its low solubility in this solvent. This compound can also be obtained by using NiCl₂·6H₂O, a Ni/ligand/azide 2:1:2 molar ratio and methanol as solvent. After filtering off the crystals of **2**, from the filtrate, crystals of compound **3** were obtained after two months. In this compound the ligand is fully deprotonated and presents the coordination mode e. The reaction of H₂L¹ with Ni(Ac)₂·4H₂O and further with NaN₃ in methanol, using a H₂L¹/ Ni^{II} /azide 1:2:2 molar ratio, led to the linear hexanuclear complex **4**, where the deprotonated ligand exhibits the coordination mode f. In view of these results, we guess that in the reaction blend H₂L¹/ Ni^{II} /azide there must be a number of available (L¹)²⁻ and (HL¹)⁻-containing Ni^{II} polynuclear complexes (including **1-4**) with subtle differences in their core. The formation of each species depend, among other factors, on the solvent and the (L¹)²⁻/(HL¹)⁻/Ni^{II}/N₃ ratio. For instance, a change in the solvent polarity could affect the deprotonation state of the ligand and could decrease/increase the nuclearity of the Ni^{II} complexes due to their different solubility.

When the ligand is allowed to react with $\text{NiCl}_2 \cdot 6\text{H}_2\text{O}$ in methanol and using a 2:1 $\text{Ni}^{\text{II}}/\text{H}_2\text{L}^1$ metal ratio, only the face-sharing defective dicubane complex **5** was obtained, in which the fully deprotonated ligand exhibit the coordination mode d. Finally, the same reaction as for **5**, but using $\text{Ni}(\text{acac})_2$ instead $\text{NiCl}_2 \cdot 6\text{H}_2\text{O}$ afforded the zig-zag trinuclear complex **6**, where the ligand acts in the coordination mode e. All these results clearly show the important role of the anionic coligand (X) in determining the final polynuclear architecture of the $(\text{L}^1)^{2-}/(\text{HL}^1)^-/ \text{Ni}^{\text{II}}/\text{X}$ system.

A summary of the different polynuclear complexes obtained from the $\text{H}_2\text{L}^1/\text{Ni}/\text{X}$ reacting systems is given in Scheme 2.

Description of the structures

The crystal structure of **1** is shown in Figure 1 and consists of Ni_2 cationic units of approximately C_2 symmetry, containing two monodeprotonated $(\text{HL}^1)^-$ bridging ligands and one $\mu_{1,1}$ -azide bridging group (end-on azide bridging group). The charge of the cationic dinuclear units is balanced by a non-coordinate azide anion. Two methanol and two water crystallization molecules are also present in the structure. Selected bond lengths and angles for **1** are given in Table S2.

The monodeprotonated ligand uses the two amine nitrogen and two phenolic oxygen atoms (one acting in a deprotonated form and the other one in a protonated form) for metal coordination. Each of the protonated phenolic oxygen atoms is monocoordinated to Ni^{II} ions, whereas the deprotonated counterparts bridge the Ni^{II} atoms. Therefore the ligand acts in a $1\kappa\text{-O}_{3\text{A}}, 1\kappa^2\text{-N}, \text{N}', 1\kappa\text{-O}_{1\text{A}}:2\kappa\text{-O}_{1\text{A}}$ -tetradentate bridging form ($\text{O}_{3\text{A}}$ represents the phenol oxygen atom), giving rise to a rather symmetrical diphenoxido- $\mu_{1,1}$ -azide-bridging fragment (mode 1c, scheme 1). The $\mu_{1,1}$ -azide bridging group with an acute Ni-N-Ni angle of 83.42° , forces the $\text{Ni}(\text{O})_2\text{Ni}$ fragment to be rather folded with a hinge angle of 52.99° (the hinge angle, β , is the dihedral angle between the two O-Ni-O planes in the bridging fragment). Owing to the folding of the structure, the $\text{Ni}\cdots\text{Ni}$ distance and Ni-O-Ni bridging angles show relatively low values of $2.8129(6)$ Å and $\sim 86.7^\circ$, respectively. The mean values of the out-of-plane displacements of the O-C bonds belonging to the phenoxido bridging groups from the Ni-O-Ni plane are 29.4° and 27.8° .

The NiN_3O_3 coordination environment displays a distorted octahedral geometry, where the three nitrogen atoms from the amine groups and the azide bridging ligand, and

2014/07/15

consequently the three oxygen atoms belonging to protonated monocoordinated phenolic group and the deprotonated phenoxido bridging groups, occupy *mer* positions. In each ligand, the phenolic oxygen atoms, deprotonated and protonated, are mutually *trans*.

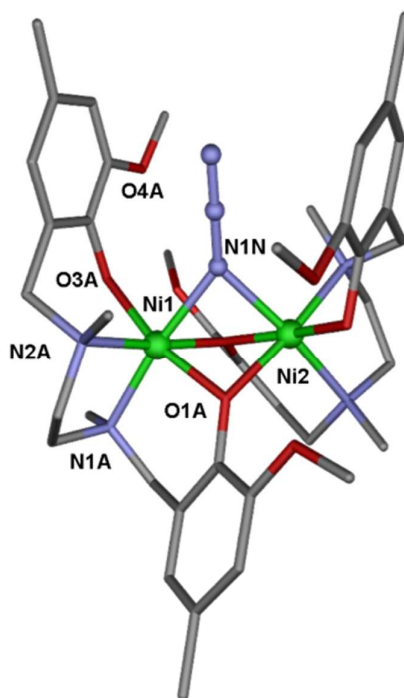


Figure 1. Perspective view of the molecular structure of **1**. Nickel, oxygen, nitrogen and carbon atoms are in light green, red, light blue and grey, respectively. Azide counteranion, hydrogen atoms and solvent molecules are omitted for the sake of clarity.

The Ni-N and Ni-O distances are found in the ranges 2.077(3)-2.118(3) and 2.024(2)-2.138(2) Å, respectively, the Ni-O distance for protonated phenolic groups being significantly larger than that for deprotonated phenoxido groups, as expected. The variation in angles between *trans* donor atoms at the metal center is small (8°) but the variation in cisoid angles spans a wide range 76.60(11)-100.38(10)° for Ni1 and 77.31(10)-100.01(11)° for Ni2.

Within the dinuclear Ni₂ unit, the protonated phenolic group of a ligand and the oxygen atom of the methoxy group of the other ligand are involved in moderate hydrogen bond interactions with O...O distances of 2.836 and 2.760 Å, thus confirming the protonated nature of the monocoordinated phenolic group. The coordinated and non-coordinated azide groups, as well as the methanol and water molecules form moderate hydrogen bonds with donor-acceptor distances in the range 2.677-2.984 Å. It should be noted that there are not intermolecular hydrogen bonds interactions connecting two dinuclear Ni₂ units.

Compound **2** is formed by a anionic tetranuclear $[\text{Ni}_2\text{Na}_2(\mu\text{-L}^1)_2(\mu_3\text{-N}_3)_2(\text{CH}_3\text{OH})(\text{N}_3)]^-$ unit and a dinuclear cationic $[\text{Ni}_2(\mu\text{-HL}^1)_2(\mu\text{-N}_3)]^+$ unit. A perspective view of the structure is given in Figure 2, whereas selected bond lengths and angles are given in Table S2.

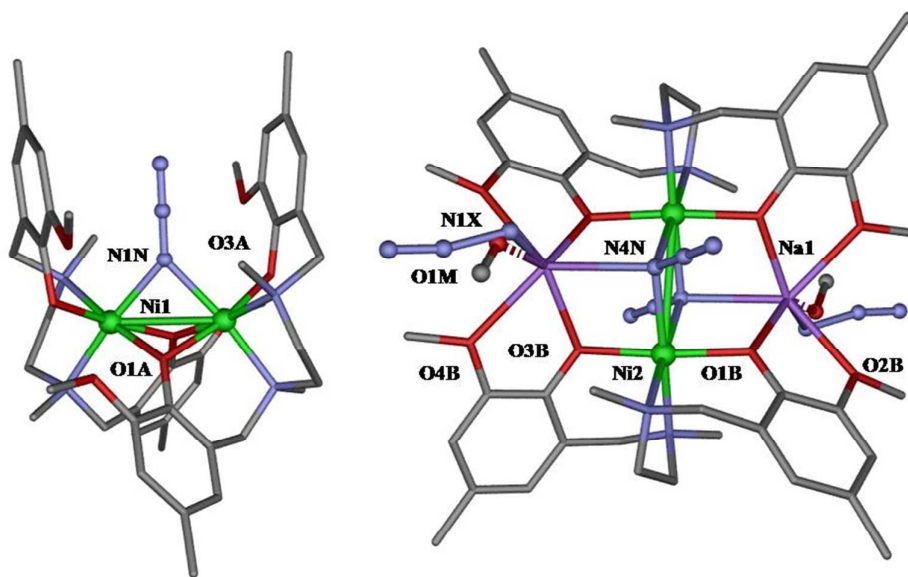


Figure 2. Perspective view of the molecular structure of **2**. Nickel, sodium, oxygen, nitrogen and carbon atoms are in light green, violet, red, light blue and grey, respectively. Disordered azide and methanol are represented at the Na1 position. Hydrogen atoms and solvent molecules are omitted for the sake of clarity.

The dinuclear unit is analogue to that of compound **1** but exhibiting a strict C_2 symmetry, the two fold-axis passing through the $\mu_{1,1}$ -azide bridging ligand. The structural parameters are very close to those observed for **1**, with Ni-N_{azide}-Ni and the Ni-O-Ni angles of $84.52(12)^\circ$ and $85.82(7)^\circ$, respectively, and the Ni \cdots Ni distance of $2.8081(8)$ Å. The mean value of the out-of-plane displacements of the O-C bond belonging to the phenoxido bridging group from the NiONi plane is 31.07° .

Within this dinuclear Ni₂ unit, the protonated phenolic group of a ligand and the oxygen atom of the methoxy group of the other ligand are involved in moderate hydrogen bond interactions with O \cdots O distance of 2.748 Å

The heterometallic Ni₂Na₂ unit exhibits a face-sharing defective dicubane-like core with two missing vertexes (Figure 2), in which two distorted octahedral Ni atoms, two Na atoms with a very distorted six-coordinated polyhedron, two deprotonated $(L^1)^{2-}$ ligands exhibiting a $1\kappa\text{-O}_{2B}, 1\kappa\text{-O}_{1B}:2\kappa\text{-O}_{1B}, 2\kappa^2\text{-N,N}', 1\kappa\text{-O}_{3B}:2\kappa\text{-O}_{3B}, 1\kappa\text{-O}_{4B}$ hexadentate

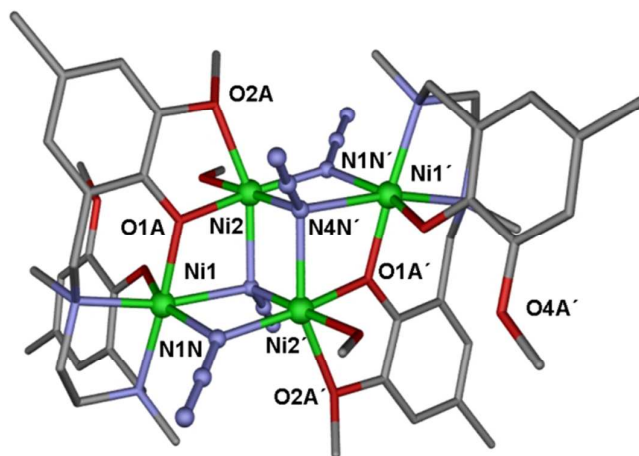
2014/07/15

bridging mode (O_2 and O_4 represent the methoxy oxygen atoms), two $\mu_{1,1,1}$ -azide bridging groups and two coordinated methanol molecules are present. The crystallographically related $Ni2$ and $Ni2'$ atoms and $N4$ and $N4'$ nitrogen atoms of the $\mu_{1,1,1}$ -azide bridging groups occupy the four vertices of the common face of the dicubane unit. The Ni atom shows a NiN_4O_2 coordination environment, which is made from the two amine nitrogen atoms of the ligand, two nitrogen atoms from the azide bridging groups, and two oxygen atoms belonging to the phenoxido-bridging groups of two different ligands connecting Na^I and Ni^{II} atoms, which occupy *trans* positions on the tetragonally compressed octahedral Ni^{II} coordination sphere (the Ni-O distances of ~ 2.03 Å are more than 0.1 Å shorter than the Ni-N distances in the equatorial plane). The Na^I ions display a very distorted environment which is made of the two methoxy and two phenoxo oxygen atoms of the two crystallographically related L_1^{2-} ligands, one methanol molecule disordered with an azide anion and the nitrogen atom of one of the μ_3 -end-on azide bridging group, with Na-X distances ($X = N$ or O) in the range 2.265(2)-2.550(3) Å. The high distortion of the NaO_5N arrangement could be due to both the non-directional nature of the electrostatic bonds and to the rigidity of the Ni_2L_2 skeleton. Each $\mu_{1,1,1}$ -azide bridging group connecting the two Ni^{II} ions and one Na^I give rise to Ni-N-Ni angles of $101.35(4)^\circ$, the azide ligand being tilted 45° from the $Ni(N)_2Ni$ plane. It should be noted that cocrystallization of two different complexes in the same compound, as it has been shown to occur in **2**, is a rather unusual fact. Nevertheless, some examples of cocrystallized Ni^{II} complexes have been reported in recent years.²¹

Compound **3** exhibits a centrosymmetric face-sharing defective dicubane-like structure, in which two vertices are missed. Within the cluster, Ni^{II} ions are connected by two phenoxido groups belonging to two deprotonated $(L^1)^{2-}$ ligands, two $\mu_{1,1,1}$ - N_3 and two $\mu_{1,1,1}$ - N_3 bridging groups. The common face of the defective dicubane unit is formed by two crystallographically related $Ni2$ and $Ni2'$ atoms and the $N4N$ and $N4N'$ nitrogen atoms of the $\mu_{1,1,1}$ -azide bridging groups. The dideprotonated ligand uses, in its coordination to the Ni^{II} ions, the two amine nitrogen atoms, the two phenoxido oxygen atoms, which bridge $Ni1$ and $Ni2$ atoms and occupy vertices of the dicubane core, and one of the methoxy oxygen atoms, thus exhibiting a $1\kappa-O_{2A}$, $1\kappa^2-N$, N' , $1\kappa-O_{1A}$: $2\kappa-O_{1A}$, $2\kappa-O_{4A}$ pentadentate bridging coordination mode (mode e in Scheme 1). In addition to the phenoxido bridge, the metal centers ($Ni1$ and $Ni2$) are also bridged by a $\mu_{1,1,1}$ -azide group, whereas the $Ni1$ and $Ni2'$ atoms are also bridged by a $\mu_{1,1}$ -azide group. The $Ni1-O1-Ni2$, $Ni1-N1N-Ni2$, $Ni1-N4N-N2$,

Ni1-N4N-Ni2' and Ni2-N4N-Ni2' bridging angles are 108.64(14)°, 102.08(15)°, 101.10(14)°, 94.52(13)° and 92.84(13)°, respectively.

The coordination spheres around both types of Ni are completed as follows. The Ni1 atom shows a NiN₄O₂ coordination environment formed by the two amine nitrogen atoms (N1A and N2A), the two oxygen atoms (O1A and O3A) belonging to monocoordinated and bridging phenoxido groups of the same ligand (L¹)²⁻ and the N1N and N4N nitrogen atoms of the $\mu_{1,1}$ -N₃ and $\mu_{1,1,1}$ -N₃ bridging groups. The Ni2 atom exhibits a NiN₃O₃ coordination environment formed by the N1N, N4N and N4N' nitrogen atoms of the $\mu_{1,1}$ -N₃ and $\mu_{1,1,1}$ -N₃ bridging groups, and the O2A, O1A and O1M oxygen atoms belonging to the coordinated methoxy group, the phenoxido bridging group and the coordinated methanol molecule, respectively. The Ni-O distances are in the range 1.956(3)-2.195(3) Å, while the Ni-N distances are in the range 2.047(4)-2.164(4) Å, see Table S2. The mean value of the out-of-plane displacement of the O-C bonds belonging to the phenoxido bridging groups from the Ni1(O1A)Ni2 plane is 18.47°, whereas the displacement of the $\mu_{1,1}$ -N₃ and $\mu_{1,1,1}$ -N₃ bridging groups with respect to the Ni1(N1N)Ni2' and Ni1(N4N)Ni2' mean planes are 13.44° and 46.62°, respectively, and those of the $\mu_{1,1,1}$ -N₃ from the Ni2(N4N)Ni2' and Ni1(N4N)Ni2 planes are 48.78° and 49.8°. The Ni1(O1A)(N4N)Ni2 and Ni1(N4N)(N1N)Ni2' bridging fragments are not planar but slightly folded with dihedral angles of 21.17° and 10.03°, respectively. The Ni2...Ni2', Ni1...Ni2 and Ni1...Ni2' intracuster distances are 3.091, 3.202 and 3.320 Å, respectively. The shortest intercluster Ni...Ni distance is 8.368 Å. There exist a moderate intramolecular hydrogen bond interaction involving the coordinated methanol molecule and the monocoordinated oxygen phenolic atom with a O...O distance of 2.568 Å.



2014/07/15

Figure 3. Perspective view of the molecular structure of **3**. Nickel, oxygen, nitrogen and carbon atoms are in light green, red, light blue and grey, respectively. Hydrogen atoms and solvent molecules are omitted for the sake of clarity.

The compound **4** shows centrosymmetric linear hexanuclear structure (Na_2Ni_4), the Na atoms being located at the ends of the molecule. This unique hexanuclear structure is made from two NaNi_2 trinuclear units connected by a double $\mu_{1,1}\text{-N}_3$ group. Within each trinuclear unit, Ni^{II} atoms are linked by a phenoxido/ $\mu_{1,1}\text{-N}_3$ /syn-syn acetate triple bridge. The ligand acts in a fully deprotonated $1\kappa\text{-O}_{2\text{A}}$, $1\kappa\text{-O}_{1\text{A}}:2\kappa\text{-O}_{1\text{A}}$, $2\kappa\text{-N}$, N' , $2\kappa\text{-O}_{3\text{A}}:3\kappa\text{-O}_{3\text{A}}$, $3\kappa\text{-O}_{4\text{A}}$ hexadentate bridging form (mode f in scheme1). Both crystallographically independent Ni^{II} atoms exhibit a NiN_3O_3 coordination sphere, which is formed, in the case of the Ni1 atom, by the two nitrogen amine atoms, the oxygen atoms O1A and O3A belonging to the two phenoxido-bridging groups, the O1B oxygen atom from the *syn-syn* acetate group and the N1N atom of the $\mu_{1,1}$ -azide bridge. The N atoms, and consequently the O atoms, are in *mer* disposition. The Ni2 atom is surrounded by the O3A phenoxido oxygen atom, the coordinated methoxy oxygen atom (O4A) and the O2B oxygen atom belonging to the carboxylate group, which are in *fac* disposition, whereas the nitrogen atoms N1N, N4N and N4N' of the three $\mu_{1,1}$ -azide bridges occupy the remaining *fac* positions. The $\text{Ni}_2(\text{N}_4\text{N})(\text{N}_4\text{N}')\text{Ni}_2'$ bridging fragment is planar but $\text{Ni}_1(\text{O}_3\text{A})(\text{N}_1\text{N})\text{Ni}_2$ bridging fragment is folded with a dihedral angle between the planes formed by $\text{N}_1\text{N}\text{Ni}_2\text{O}_3\text{A}$ and $\text{O}_3\text{A}\text{Ni}_1\text{N}_1\text{N}$ atoms of 28.59° . The $\text{Ni}_1(\text{O}_3\text{A})\text{Ni}_2$ and $\text{Ni}_2(\text{N}_1\text{N})\text{Ni}_1$ bridging angles are $95.55(16)^\circ$ and $92.6(2)^\circ$, respectively, whereas the $\text{Ni}_1\cdots\text{Ni}_2$ distance is 3.04 \AA . The mean value of the out-of-plane displacements of the O-C bonds belonging to the phenoxido bridging groups from the $\text{Ni}_1(\text{O}_3\text{A})\text{Ni}_2$ plane is 61.29° , whereas the deviation of the end-on bridging group with respect to the $\text{Ni}_1(\text{N}_1\text{N})\text{Ni}_2$ is 42.91° . The $\text{Ni}_2(\text{N}_4\text{N})\text{Ni}_2$ bridging angle and the $\text{Ni}_2\cdots\text{Ni}_2'$ distance are $101.1(2)^\circ$ and 3.198 \AA .

The Na atom shows a NaO_5 coordination environment with a distorted square-pyramidal geometry. In this description the basal plane is formed by the oxygen atoms belonging to the phenoxido bridging group (O1A) and the methoxy group (O2A) of the ligand, the molecule of methanol (O2M) and the acetate bridging group (O1B). The axial position is occupied by the oxygen atom of the other methanol molecule (O1M). The average distance in the basal plane is 2.325 \AA , whereas the apical distance is $2.172(15) \text{ \AA}$.

The deviation of Na atom from this basal plane is 0.511 Å. The shortest Ni...Ni intermolecular distance is 9.963 Å.

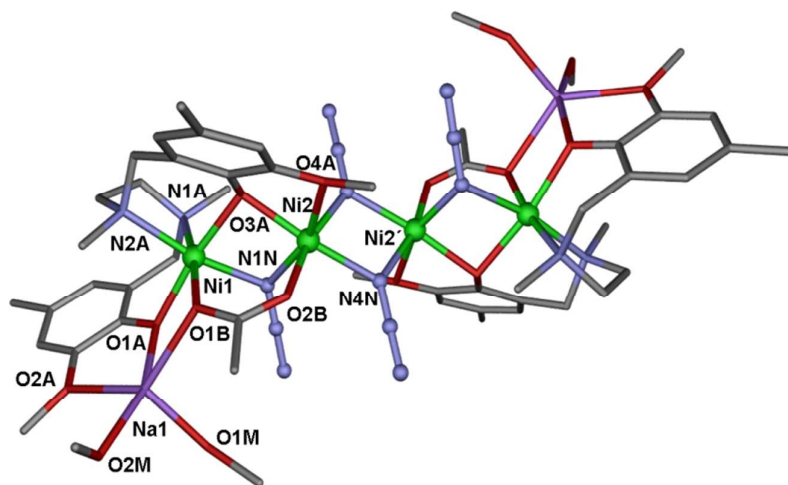


Figure 4. Perspective view of the molecular structure of **4**. Nickel, sodium, oxygen, nitrogen and carbon atoms are in light green, violet, red, light blue and grey, respectively. Hydrogen atoms are omitted for the sake of clarity.

The structure of **5** is given in Figure 5 whereas selected bond distances and angles are listed in Table S2. As observed for **3**, the structure of compound **5** consists of centrosymmetric face-sharing defective dicubane-like neutral molecules. Two types of octahedrally coordinated Ni atoms, Ni1 and Ni2, can be distinguished. The crystallographically related Ni1 and Ni1' occupy two vertices of the common face of the dicubane unit and are connected by two μ_3 -chloride bridging ligands with Ni1-Cl1-Ni1' bridging angles of 90.27(16)° and a Ni1...Ni1' distance of 3.531 Å. Ni2 and Ni2' ions occupying the outer part of the Ni₄ molecule, are connected to the central Ni1 and Ni1' ions through two non-equivalent μ -phenoxido/ μ_3 -Cl double bridges with Ni2-Cl-Ni1 and Ni2-O-Ni1 bridging angles of 86.06(17)° and 113.4(5)° for a bridging fragment and 85.01(17)° and 112.6(7)° for the other one. The corresponding Ni1...Ni2 distances for these almost planar bridging fragment are 3.372 Å and 3.352 Å, respectively. The fully deprotonated ligand exhibits a symmetrical 2 κ -O_{4A}, 2 κ -O_{1A}:1 κ -O_{1A}, 2 κ^2 -N, N', 2 κ -O_{3A}:3 κ -O_{3A}, 1 κ -O_{4A} hexadentate bridging mode (mode d in scheme 1). Besides the presence of μ_3 -Cl groups instead of μ_3 -azide groups connecting the Ni ions of the central bridging fragment, the most significant difference between **3** and **5** is the existence of μ -X/ μ -phenoxido and μ_3 -X/ μ -phenoxido double bridges connecting the central and outer Ni ions in the former (X = azide),

2014/07/15

instead of the two $\mu_3\text{-X}/\mu\text{-phenoxido}$ found in the latter ($\text{X} = \text{chloride}$). The central Ni1 atoms show a $\text{NiN}_2\text{O}_2\text{Cl}_2$ distorted octahedral coordination environment, which is formed by two *cis*-amine nitrogen atoms and two *trans*-phenoxido-bridging oxygen atoms of the $(\text{L}^1)^{2-}$ ligand and two *cis*- $\mu_3\text{-Cl}$ monoatomic ligands. The outer Ni2 atoms displays a NiO_4Cl_2 coordination sphere which is made from four oxygen atoms, two of them belonging to the phenoxido-bridging group and the other two belonging to monocoordinated methoxy groups of the ligand (both couples of ligands adopt a *cis* disposition), whereas the remaining positions are occupied by one $\mu_3\text{-Cl}$ ligand and one monocoordinated Cl ligand. The Ni-O, Ni-N and Ni-Cl bond distances are in the ranges 1.989(12)-2.347(10) Å, 2.105(12)-2.132(16) Å and 2.278(6)-2.501(4) Å, respectively. The mean values of the out-of-plane displacements of the O-C bonds belonging to the phenoxido bridging groups from the Ni1Ni2 plane are 29.66° and 33.1° . Tetranuclear molecules of **5** are well isolated in the structure, the shortest intercluster $\text{Ni}\cdots\text{Ni}$ distance being of 7.622 Å.

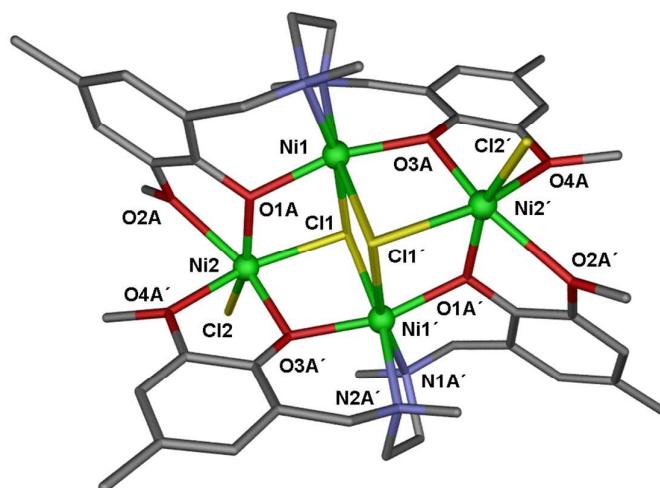


Figure 5. Perspective view of the molecular structure of **5**. Nickel, Chlorine, oxygen, nitrogen and carbon atoms are in light green, yellow, red, light blue and grey, respectively. Hydrogen atoms are omitted for the sake of clarity.

Compound **6** is made of unique bent trinuclear entities with C_2 symmetry, in which the central and outer Ni^{II} ions are bridged by single phenoxido bridging groups (Figure 6). The fully deprotonated $(\text{L}^1)^{2-}$ ligand adopts a $2\kappa\text{-O}_{2\text{A}}, 2\kappa\text{-O}_{1\text{A}}:1\kappa\text{-O}_{1\text{A}}, 2\kappa^2\text{-N}, \text{N}', 1\kappa\text{-O}_{3\text{A}}$ pentadentate coordination mode, with single-bridging and monocoordinated phenoxido groups and uncoordinated and monocoordinated methoxy groups. The central Ni2 atom exhibit a distorted octahedral NiO_6 coordination sphere, which is formed by two coordinated water molecules in *cis* disposition and two methoxy and two phenoxido-bridging oxygen

atoms (in *trans* disposition) belonging to two different $(L^1)^{2-}$ ligands. The octahedrally distorted NiN_2O_4 coordination environment of Ni1, is made from two amine nitrogen atoms, one monocoordinated phenoxido oxygen atom (O3A) and the phenoxido-bridging oxygen atom (O1A) of the deprotonated $(L^1)^{2-}$ ligand, whereas the other two remaining positions are occupied by the oxygen atoms of an acetylacetonate bidentate ligand. The Ni-O distances are in the ranges 2.015(2)-2.110(2) and 2.018(2)-2.090(2) Å for Å for Ni1 and Ni2, respectively (selected bond angles are given in Table S2). The mean value of the out-of-plane displacement of the O-C bonds belonging to the phenoxido bridging groups from the Ni1(O1A)Ni2 plane is 18.13°. It should be noted that each molecule of water is involved in a trifurcated four-centered hydrogen bond with the oxygen atoms belonging to the uncoordinated methoxy group, the monocoordinated phenoxido group and one of the oxygen atoms of the bidentate acetylacetonate ligand with $O\cdots O$ donor acceptor distances of 2.843 Å, 2.727 Å and 2.699 Å, respectively (Figure S1, ESI). These moderate intramolecular hydrogen bond interactions are ultimately responsible for the bent conformation of the Ni_3 molecules. Ni_3 molecules are well isolated in the structure, the shortest $Ni\cdots Ni$ intertrinnuclear distance being of 8.973 Å.

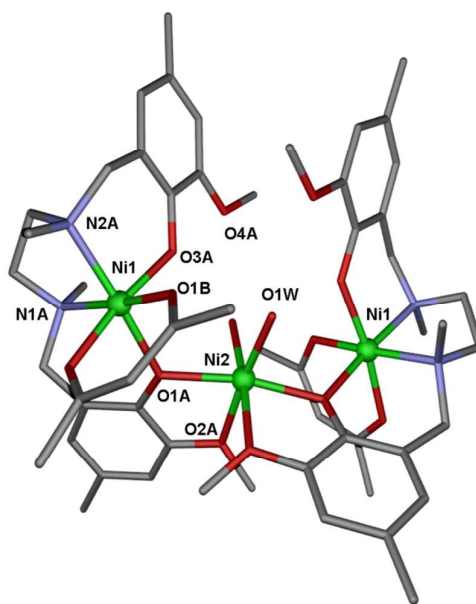


Figure 6. Perspective view of the molecular structure of **6**. Nickel, oxygen, nitrogen and carbon atoms are in light green, red, light blue and grey, respectively. Hydrogen atoms are omitted for the sake of clarity.

Magnetic Properties

2014/07/15

The temperature dependence of the magnetic properties of powdered polycrystalline samples of **1-6** under a constant magnetic field of 0.1 T in the 2–300 K range are represented in the form $\chi_M T$ vs T plots (χ_M being the molar paramagnetic susceptibility of the compound) in Figures 7-12, respectively.

The $\chi_M T$ values at room temperature for **1**, **2**, **3** and **4** (2.65 cm³mol⁻¹K, 5.23 cm³mol⁻¹K, 5.88 cm³mol⁻¹K and 5.35 cm³mol⁻¹K respectively) are significantly higher than those expected for uncoupled Ni²⁺ ions ($S = 1$) with $g = 2.0$ (2.0 cm³mol⁻¹K for **1** and 4.0 cm³mol⁻¹K for **2** and **4**), which is mainly due to the orbital contribution of the Ni^{II} ions. When the temperature is lowered, the $\chi_M T$ for complexes **1**, **2**, **3** and **4** steadily increases reaching a maximum at 25 K (3.48 cm³mol⁻¹K), 15 K (6.91 cm³mol⁻¹K), 10 K (11.48 cm³mol⁻¹K) and 9 K (11.16 cm³mol⁻¹K), respectively. Below the temperature of the maximum, the $\chi_M T$ decreases down to 2 K to reach values of 2.95 cm³mol⁻¹K, 5.84 cm³mol⁻¹K, 8.78 cm³mol⁻¹K and 9.36 cm³mol⁻¹K for **1**, **2**, **3** and **4**, respectively. This behaviour confirms the existence of significant intramolecular ferromagnetic couplings between the Ni^{II} ions leading to a $S = 2$ ground state in **1**, two $S = 2$ ground states in **2** and a $S = 4$ ground state for **3** and **4**. The decrease in $\chi_M T$ at low temperatures is more likely due to zero-field splitting effects (ZFS) of the ground state and/or intermolecular antiferromagnetic interactions.

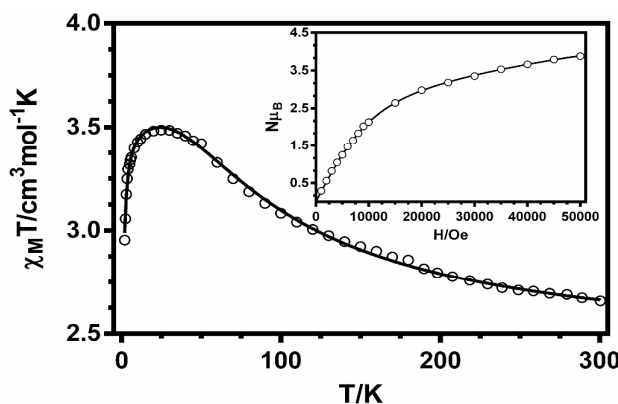


Figure 7. Temperature dependence of $\chi_M T$ for **1**. The solid line is generated from the best fit to the magnetic parameters. Inset: Field dependence of the magnetization for **1**. The black solid line represents a simulation with the parameters extracted from the best fit of the magnetic susceptibility data.

The magnetic properties of **1** have been modelled by using the following Hamiltonian:

$$H = -JS_{Ni1}S_{Ni2} + \sum_{i=1}^2 D_{Ni}S_{Niz}^2$$

where J accounts for the magnetic exchange coupling between the Ni²⁺ ions and D_{Ni} accounts for the axial single ion zero-field splitting parameter of the Ni^{II} ions (D_{Ni} is

assumed to be the same for both Ni^{2+} ions). The fit of the experimental susceptibility data with the above Hamiltonian using the full-matrix diagonalization PHI program²² afforded the following set of parameters: $J = +46.9 \text{ cm}^{-1}$, $g = 2.16$ and $D = 4.9 \text{ cm}^{-1}$ ($R = 8.4 \times 10^{-7}$ ($R = \Sigma[(\chi_{\text{M}}T)_{\text{exp}} - (\chi_{\text{M}}T)_{\text{calcd.}}]^2 / \Sigma(\chi_{\text{M}}T)_{\text{exp}}^2$)). As expected, similar values were obtained with negative values of D , but the quality of the fit got worse (see ESI). The D_{Ni} values are in agreement with the expected single-ion values reported in the literature.²³ When D_{Ni} was fixed to zero and a term accounting for the intermolecular interactions by means of the molecular field approximation, $-zJ' \langle S_z \rangle S_z$, was introduced in the Hamiltonian, the fit led to the slightly different magnetic parameters: $J = +40.9 \text{ cm}^{-1}$, $g = 2.18$ and $zJ' = -0.067 \text{ cm}^{-1}$ ($R = 5.5 \times 10^{-7}$). As usual, the extracted J value when $zJ' = 0$ is higher than that extracted for $D = 0$. It should be noted that the D_{Ni} values obtained with $zJ' = 0$ and the zJ' values obtained with $D_{\text{Ni}} = 0$ can be considered as the limit values for these parameters, as zJ' and D_{Ni} are strongly correlated and provoke the same result at low temperature. Therefore, these parameters cannot be accurately determined by the fit of the magnetic data. Hereafter, for all the compounds we will keep the data extracted with zJ' fixed to zero for discussions and comparative purposes.

In keeping with the structure of **2**, we have analyzed the data of this compound with the Hamiltonian

$$H = -J S_{\text{Ni}1} S_{\text{Ni}2} - J_1 S_{\text{Ni}3} S_{\text{Ni}4} + \sum_{i=1}^4 D_{\text{Ni}} S_{\text{Ni}i}^2 - zJ' \langle S_z \rangle S_z$$

where J and J_1 are the magnetic exchange couplings through the (diphenoxido)($\mu_{1,1}$ - N_3) and double ($\mu_{1,1}$ - N_3) bridging fragments of the Ni_2 and Na_2Ni_2 units, respectively, and zJ' accounts for the intermolecular interactions using the molecular field approach. D_{Ni} is assumed to be the same for the two types of Ni^{2+} ions that are present in the structure. As indicated above, D and zJ' are closely related and their independent contributions cannot be accurately determined from the fit of the magnetic data. Therefore, we have fixed to zero either zJ' or D . For zJ' fixed to zero, the fit of the experimental susceptibility data with the above Hamiltonian using the full-matrix diagonalization PHI program²² afforded the following set of parameters: $J = +53.1 \text{ cm}^{-1}$, $J_1 = +26.5 \text{ cm}^{-1}$, $g = 2.16$ and $D = 5.07 \text{ cm}^{-1}$ with $R = 3.3 \times 10^{-6}$. As in the case of **1**, similar values were obtained with negative values of D , but the quality of the fit got worse (see ESI).

2014/07/15

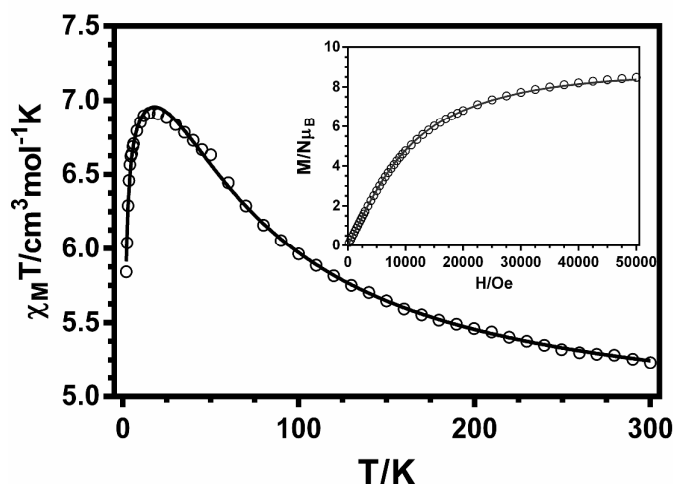


Figure 8. Temperature dependence of $\chi_M T$ for **2**. The solid line is generated from the best fit to the magnetic parameters. Inset: Field dependence of the magnetization for **2**. The black solid line represents a simulation with the parameters extracted from the best fit of the magnetic susceptibility data.

The field dependences of the molar magnetization at 2 K for compounds **1** and **2** (inset Figure 7 and 8) match well with the curves generated with the magnetic parameters extracted from the best fit of the magnetic susceptibility data.

The experimental susceptibility data for **3**, with a centrosymmetric face-sharing defective dicubane-like structure, were modelled with the following three- J Hamiltonian (see inset Figure 9):

$$H = -J_1(S_{Ni1}S_{Ni2} + S_{Ni1'}S_{Ni2'}) - J_2(S_{Ni1}S_{Ni2'} + S_{Ni1'}S_{Ni2}) - J_3(S_{Ni2}S_{Ni2'})$$

where J_1 , J_2 and J_3 describe the exchange pathways through the μ -phenoxido/ $\mu_{1,1,1}$ -azide, $\mu_{1,1}$ -azide/ $\mu_{1,1,1}$ -azide and $\mu_{1,1,1}$ -azide/ $\mu_{1,1,1}$ -azide, respectively. The D parameter accounting for the local anisotropy of the Ni^{II} ions was not included in the Hamiltonian to avoid overparametrization. In consequence, only data above 25 K, which are not affected by the effects of D , were fitted with the above Hamiltonian. The best fit led to the following set of parameters: $J_1 = +33.5 \text{ cm}^{-1}$, $J_2 = +2.0 \text{ cm}^{-1}$, $J_3 = +17.4 \text{ cm}^{-1}$ and $g = 2.23$ with $R = 2.1 \times 10^{-4}$.

The defective-cubane core of **3** exhibits three magnetic exchange pathways: (i) double- $\mu_{1,1,1}$ -azide, (ii) double $\mu_{1,1,1}$ -azide/ $\mu_{1,1}$ -azide and (iii) double μ -phenoxido/ $\mu_{1,1,1}$ -azide.

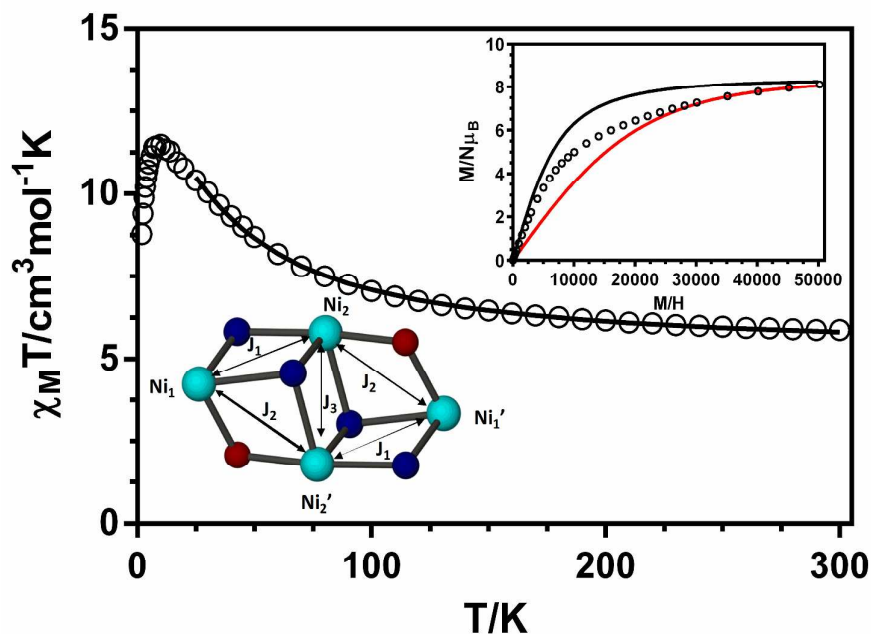


Figure 9. Temperature dependence of $\chi_M T$ for **3**. The solid line is generated from the best fit to the magnetic parameters. Inset top: Field dependence of the magnetization for **3**. The black and red solid lines represent Brillouin functions for an $S = 4$ ground state and for the sum of four Ni^{II} ions with $S = 1$, respectively. Inset bottom: Magnetic exchange pathways in compound **3**.

According to the structure of compound **4**, the susceptibility data were modeled with the following two- J Hamiltonian (see inset Figure 10):

$$H = -J_1(S_{\text{Ni}1}S_{\text{Ni}2} + S_{\text{Ni}1'}S_{\text{Ni}2'}) - J_2(S_{\text{Ni}2}S_{\text{Ni}2'})$$

where J_1 and J_2 describe the magnetic exchange pathways through the triple bridge μ -phenoxido/ $\mu_{1,1}$ -azide/ μ -syn-syn acetate and double $\mu_{1,1}$ -azide bridge, respectively. In order to avoid overparametrization we have fitted the data above 20 K to eliminate the effect of the anisotropy and possible intermolecular interactions. The best fit parameters were: $J_1 = +28.8 \text{ cm}^{-1}$, $J_2 = +81.9 \text{ cm}^{-1}$ and $g = 2.11$ with $R = 5 \times 10^{-5}$.

2014/07/15

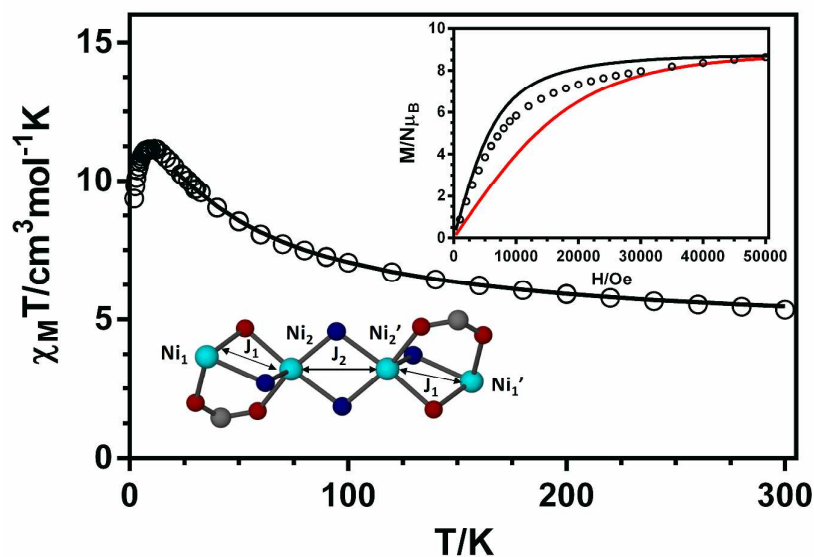


Figure 10. Temperature dependence of $\chi_M T$ for **4**. The solid line is generated from the best fit to the magnetic parameters. Inset top: Field dependence of the magnetization for **4**. The black and red solid lines represent Brillouin functions for an $S = 4$ ground state and for the sum of four Ni^{II} ions with $S = 1$, respectively. Inset bottom: Magnetic exchange pathways in compound **4**.

The field dependence of the molar magnetization at 2 K for compounds **3** and **4** are given (inset Figures 9 and 10), is above the Brillouin function for the sum of the contribution of four isolated Ni^{II} ions (red lines), which corroborates the existence of ferromagnetic interaction between the Ni^{2+} ions. However, the experimental data are below the Brillouin function for a $S = 4$ ground state, which is due to the presence of significant anisotropy and possible intermolecular interactions.

The $\chi_M T$ values at room temperature for complexes **5** and **6** (4.76 and $3.40 \text{ cm}^3 \text{ mol}^{-1} \text{ K}$, respectively) are close to those expected for four and three uncoupled Ni^{II} ions ($S = 1$) with $g = 2.0$ (4.0 and $3.0 \text{ cm}^3 \text{ mol}^{-1} \text{ K}$, respectively). As can be observed in Figures 11 and 12, the $\chi_M T$ product remains almost constant for **5** until 40 K and decreases with decreasing temperature until ~ 75 K for **6**, respectively. Below these temperatures, the $\chi_M T$ product sharply decreases to reach a value of $0.87 \text{ cm}^3 \text{ mol}^{-1} \text{ K}$ at 2 K for **5** and a quasi plateau at 5 K of $1.2 \text{ cm}^3 \text{ mol}^{-1} \text{ K}$ for **6**. For the latter complex, the $\chi_M T$ decreases again down to a value of $0.85 \text{ cm}^3 \text{ mol}^{-1} \text{ K}$ at 2 K (see inset Figure 12). This behaviour suggests the existence of a weak to moderate global antiferromagnetic interaction in both compounds leading to $S = 0$ and $S = 1$ ground states for **5** and **6**, respectively. The fact that $\chi_M T$ value for **6** at 2 K is

lower than that expected for a triplet state ($\sim 1 \text{ cm}^3 \text{ mol}^{-1} \text{ K}$) is due to the existence of significant zero-field splitting effects promoted by the local anisotropy of the Ni^{II} ions, which are the main factor responsible of the decrease $\chi_{\text{M}}T$ at very low temperature.

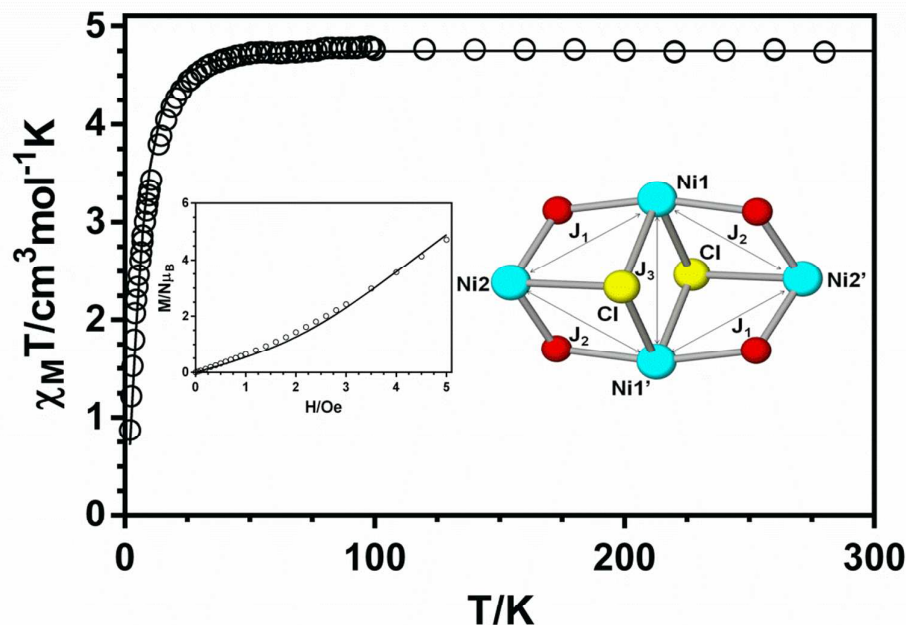


Figure 11. Temperature dependence of $\chi_{\text{M}}T$ for **5**. The solid lines is generated from the best fit to the magnetic parameters. Inset left: Field dependence of the magnetization for **5**. The black solid line represents a simulation with the parameters extracted from the best fit of the magnetic susceptibility data. Inset right: Magnetic exchange pathways in compound **5**.

In order to know the influence of the Ni^{II} local anisotropy on the magnetic properties of Ni_4 defective cubane complex **5**, we have performed simulations with the PHI program²² on the three- J model indicated in the inset of Figure 11 (absolute D values were varied between 0 and 4 cm^{-1}). In all cases, the results of the simulations clearly show that the influence of D is a very weak effect, very difficult to evidence from the magnetic susceptibility data. This is in good accordance with the results previously reported for chain²⁴ and dinuclear Ni^{II} complexes.²⁵ In view of the above considerations and to avoid overparametrization, the magnetic data were analysed by using the following isotropic spin Heisenberg Hamiltonian, in which the local anisotropy of the Ni^{II} ions was not taken into account and J_1 and J_2 were considered to be equal:

$$H = -J_1(S_{\text{Ni}1}S_{\text{Ni}2} + S_{\text{Ni}1}S_{\text{Ni}2'}) - J_2(S_{\text{Ni}1'}S_{\text{Ni}2} + S_{\text{Ni}1}S_{\text{Ni}2'}) - J_3(S_{\text{Ni}1}S_{\text{Ni}1'})$$

2014/07/15

A good fit was obtained with the following parameters: $J_1 = 1.92 \text{ cm}^{-1}$, $J_3 = +7.2 \text{ cm}^{-1}$ and $g = 2.18$ with $R = 2.5 \times 10^{-6}$. Assuming $J_1 = J_2$, the combination of sign for J_1 and J_3 found in **5** (antiferromagnetic and ferromagnetic, respectively) does not lead to spin frustration because they are not competing interactions. The ground state is singlet for all J_1/J_3 ratios and the first excited state a triplet lying at 1.92 cm^{-1} above the ground state.

According to the bent trinuclear arrangement of Ni^{II} ions in compound **6** with C_2 symmetry (see inset Figure 12) the magnetic data have been analyzed according to the following Hamiltonian:

$$H = -J_1(S_{\text{Ni}1}S_{\text{Ni}2} + S_{\text{Ni}1}S_{\text{Ni}2'}) + \sum_{i=1}^3 D_{\text{Ni}}S_{\text{Ni}z}^2$$

where J_1 represents the magnetic couplings between the central and external Ni^{II} ions. As the trinuclear molecules are very well isolated in the structure, to take into account the decrease at very low temperature, we have considered the local anisotropy of the Ni^{II} ions (D_{Ni} is assumed to be the same for the two types of Ni^{2+} ions). The best fit led to the following parameters: $J_1 = -6.8 \text{ cm}^{-1}$, $g = 2.19$ and $D = 4.4 \text{ cm}^{-1}$ with $R = 8 \times 10^{-5}$. Similar values were obtained with negative values of D , but the quality of the fit got worse (see ESI)

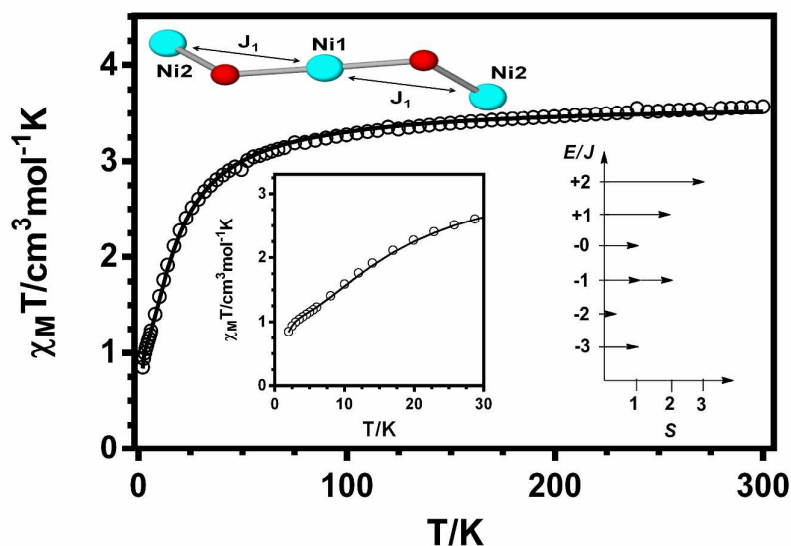


Figure 12. Temperature dependence of $\chi_M T$ for **6**. The solid line is generated from the best fit to the magnetic parameters. Inset top: Magnetic exchange pathways in compound **6**. Inset bottom left: highlight of the low temperature portion of the $\chi_M T$ vs T plot. Inset bottom right: Energy levels diagram for **6**.

The field dependence of the molar magnetization at 2 K for compounds **6** (Figure

S2 ESI), is slightly below the Brillouin function for a $S = 1$ and $g = 2.2$, thus supporting the nature of ground state. The deviation from the Brillouin function is more likely due to zero-field splitting effects. At applied magnetic field higher than 4T, the experimental points are above the Brillouin function and the magnetization does not achieve a complete saturation at 5T. This behaviour suggests the presence of low-lying excited states that are partially [thermally and field-induced] populated.

In order to support the experimental J values found for compounds **1-6**, DFT calculations using the broken-symmetry approach were carried out on the X-ray structures as found in solid state. As it can be observed in Table 1, the calculated values are in good agreement in sign and magnitude with those of the experimental results.

Table 1.- Magnetic pathways and magnetic coupling constants for complexes **1-6**.

Compound	Magnetic pathways	$J_{\text{exp}} (\text{cm}^{-1})$	$J_{\text{calc}} (\text{cm}^{-1})$
1	di- μ -phenoxido/ $\mu_{1,1}$ -azido	+46.9	+53.3
2	di- μ -phenoxido/ $\mu_{1,1}$ -azido di- $\mu_{1,1,1}$ -azido	+53.1 (J) +26.5 (J_1)	+54.3 (J) +30.3 (J_1)
3	$\mu_{1,1}$ -azido / $\mu_{1,1,1}$ -azido μ -phenoxido/ $\mu_{1,1,1}$ -azido Di- $\mu_{1,1,1}$ -azido	+33.5 (J_1) +2.0 (J_2) +17.4 (J_3)	+45.3 (J_1) +9.2 (J_2) +23.7 (J_3)
4	μ -phenoxido/(<i>syn,syn</i>) acetate/ $\mu_{1,1}$ -azido Di- $\mu_{1,1}$ -azido	+28.8 (J_1) +81.9 (J_2)	+37.1 (J_1) +83.7 (J_2)
5	μ -phenoxido / μ_3 -chloride μ -phenoxido / μ_3 -chloride Di- μ_3 -chloride	-1.92 (J_1) ^a +7.2 (J_3)	-1.26 (J_1) -12.54 (J_2) +8.75 (J_3)
6	μ -phenoxido	-6.58(J_1)	-6.3 (J_1)

J_1 and J_2 were considered to be equal.

Rationalization of the experimental magnetic properties in terms of the structural parameters.

The ferromagnetic coupling exhibited by complex **1** can be justified by analyzing the separate effects of the diphenoxido and $\mu_{1,1}$ -azide-bridging group connecting the octahedral Ni^{II} ions. Let us start with the diphenoxido-bridged $\text{Ni}(\text{O})_2\text{Ni}$ fragment. Experimental and theoretical magneto-structural correlations carried out by us²⁶ and others²⁷ have clearly shown that the Ni-O-Ni bridging angle (θ) is the main factor affecting the nature of the magnetic exchange interaction in planar hydroxido-, alkoxido- and phenoxido- $\text{Ni}(\text{O})_2\text{Ni}$ complexes. Thus, for Ni-O-Ni angles close to 90° , a ferromagnetic coupling is expected. As the Ni-O-Ni angle deviates from 90° , the ferromagnetic coupling decreases and becomes antiferromagnetic at values of $\sim 96-98^\circ$ (the AF coupling is favoured when θ increases).

2014/07/15

Moreover, it has been shown from theoretical studies²⁶ that, on the one side, the AF interaction increases when τ (the out-of-plane displacement of the phenyl carbon atom from the Ni₂O₂ plane) decreases and, on the other side, the AF increases when β decreases (hinge angle between the O-Ni-O planes in the bridging region). In view of this, it is reasonable to guess that small θ angles (in the vicinity of 90-95°) combined with larger τ (> 30-40°) and β values (> 20°) should lead to weak AF or even F interactions in diphenoxido-bridged nickel(II) complexes. Taking into account these magneto-structural correlations, the folded Ni(O)₂Ni diphenoxido-bridging fragment in complex **1**, with mean θ and τ angles of 86.7°, 28.6° and a β of 50.5° should transmit F interactions between the Ni²⁺ ions. It is well known that the $\mu_{1,1}$ -azide-bridging group generally transmits ferromagnetic interactions between the Ni²⁺ ions²⁸ and it was theoretically shown²⁹ for double $\mu_{1,1}$ -dinuclear Ni^{II} complexes that the ferromagnetic interaction reach a maximum value for $\theta = 104^\circ$ and then steadily decrease with decreasing θ . In view of the above considerations the large ferromagnetic interaction between the Ni^{II} ions observed for **1** is not unexpected.

Although numerous examples of structurally and magnetically mixed-bridged dinuclear Ni^{II} complexes exist, only in one of them the Ni^{II} ions are connected by two diphenoxido and one $\mu_{1,1}$ -azido bridging group.³⁰ This compound of formula [Ni₂L²₂($\mu_{1,1}$ -N₃)($\mu_{1,1,1}$ -N₃)]_n (HL² is a N₂O tridentate chelate Schiff base ligand) exhibits a 1D polymeric chain structure where the diphenoxido($\mu_{1,1}$ -N₃)-bridged dinickel(II) units, [Ni₂L¹₂($\mu_{1,1}$ -N₃)], are connected by $\mu_{1,1,1}$ -N₃ bridging groups. Therefore, complex **1** represents the first example of a genuine dinuclear Ni^{II} complex containing a triple diphenoxido($\mu_{1,1}$ -N₃) bridge. From the magnetic point of view, the polymeric compound [Ni₂L²₂($\mu_{1,1}$ -N₃)($\mu_{1,1,1}$ -N₃)]_n is a F/AF alternating chain with a J value for the ferromagnetic interaction mediated by the triple diphenoxido($\mu_{1,1}$ -N₃) bridge of +34.2 cm⁻¹, which is significantly smaller than those extracted compound **1**. However, the DFT calculated J value for a dinuclear model [Ni₂L¹₂($\mu_{1,1}$ -N₃)(N₃)₂], built from the crystal structure but exhibiting two terminal azide ligands, was +59 cm⁻¹, which is larger but close to that calculated for **1** of +53 cm⁻¹.

In order to know if, besides the Ni-N-Ni angle (θ), other structural parameters of the $\mu_{1,1}$ -azide bridging ligand, affect the magnitude of the magnetic coupling in this type of rare triple bridged di- μ -phenoxido- $\mu_{1,1}$ -azide dinuclear Ni^{II} unit, we have performed DFT calculations on a model compound where azide and nitrogen donor atoms of the ligands have been replaced by ammonia molecules (Figure 13). In particular, taking as starting point the X-ray structure of **1**, we have calculated the effect of the following structural factors: (i)

the variation of the Ni-N_{azide} distance with an concomitant change of the Ni-N_{azide}-Ni angle (θ) (ii) the in plane motion (rocking) with θ being constant (iii) out-of-plane (wagging) motion with θ being constant (iv) azide direct transfer where the N_{ammonia}-Ni-N_{azide} angle varies as well as one of the Ni-N_{azide} distances giving rise to an asymmetric azide bridging mode and (v) the same as iv but with the concomitant change of the Ni-N_{azide}-N_{azide} angle (azide compensated transfer). As it can be on figure 13, the increase of any of the structural parameters i-v causes a significant decrease in the magnitude of the ferromagnetic interaction.

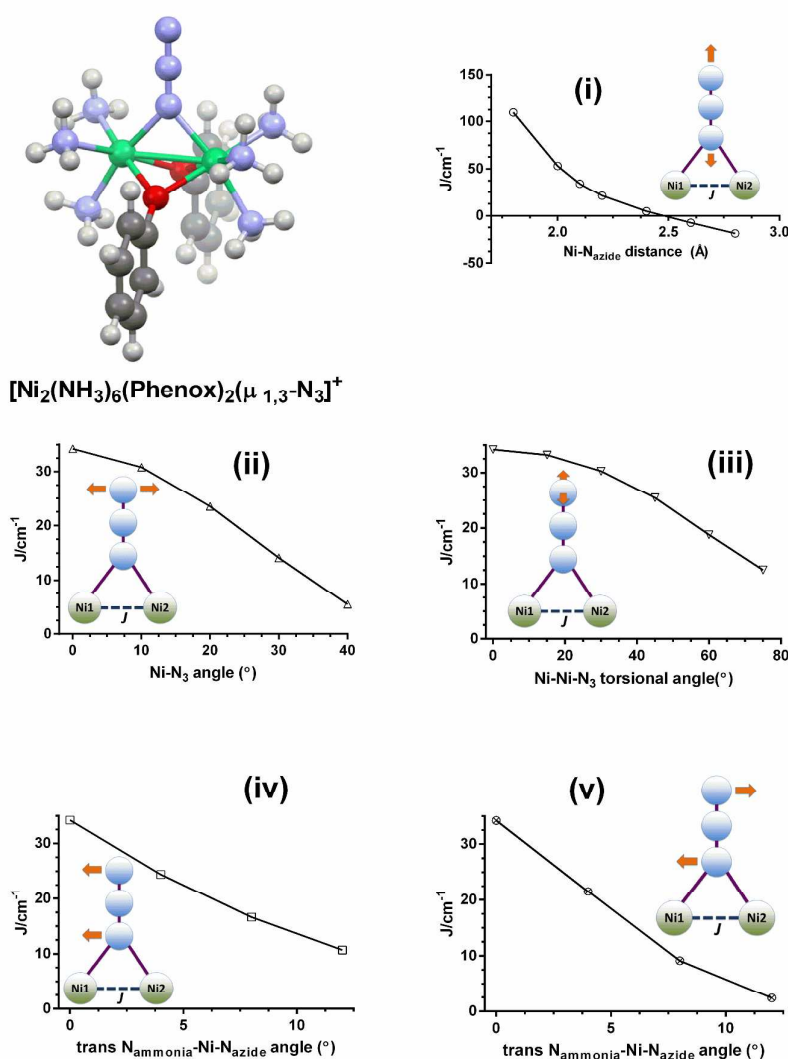


Figure 13.- (top left) model compound. (top right) (i) Dependence of J with the Ni-N_{azide} distance. (ii) Rocking motion (iii) wagging motion (iv) azide direct transfer (the azide ligand is kept perpendicular to the Ni···Ni vector) (v) azide transfer compensated (in the final position the trans NH₃-Ni-N_{azide} angle is 180 ° and azide group is colinear with the NH₃-Ni-N_{azide} axis).

2014/07/15

Compared to **1**, the Ni(O)₂Ni unit of the diphenoxido/ $\mu_{1,1}$ -azide bridging fragment of the 1D complex $[\text{Ni}_2\text{L}^1_2(\mu_{1,1}\text{-N}_3)(\mu_{1,1,1}\text{-N}_3)]_n$ has an smaller average Ni-O-Ni bridging angle (θ) and larger τ and β angles and therefore should provoke a larger ferromagnetic coupling. Beside this and with regard to the Ni-N₃-Ni fragment, the 1 D chain complex possesses a Ni-N_{azide}-Ni bridging angle $\theta = 86.11^\circ$ and structural factors (i-v) that all favour the existence of a stronger ferromagnetic interaction than in **1** (in the 1 D complex has a symmetrical Ni-N₃-N fragment, with a zero Ni-Ni-N₃ torsional angle and a Ni-N_{azide} distance of 2.092 Å that is shorter than that of **1**), which agrees well with the theoretical results. The reason why the experimental magnetic coupling for $[\text{Ni}_2\text{L}^2_2(\mu_{1,1}\text{-N}_3)(\mu_{1,1,1}\text{-N}_3)]_n$ is weaker than in **1**, may be found in the fact that the fitting of the magnetic data for the former, even good, was performed only in the 20-300 K and, moreover, it does not reproduce well the maximum observed in the $\chi_M T$ vs T plot as well as the experimental points below the temperature of the maximum. This can introduce some degree of uncertainty in the extracted J value being ultimately lower than expected. We feel, in light of the results for **1** and **2** (see below), that the magnetic coupling in this type diphenoxido($\mu_{1,1}$ -N₃)-bridged dinickel(II) unit should be above +40 cm⁻¹.

To the best of our knowledge, compound **2** represents the first example of a compound where coexist in the crystal structure two different azide-bridged dinuclear Ni^{II} units: one with diphenoxido- $\mu_{1,1}$ -N₃ and the other one with double $\mu_{1,1}$ -N₃ bridges. Within the diphenoxido($\mu_{1,1}$ -N₃)-bridged dinickel(II) unit of **2**, the θ , τ and β angles with values of 85.83°, 31.02° and 51.27°, respectively, as well as the Ni-N_{azide}-Ni angle of 84.53°, all of them favour a slightly stronger ferromagnetic interaction for this unit in **2** than in **1**, which agrees well with the experimental and calculated results.

As for the double ($\mu_{1,1,1}$ -N₃)-bridged unit, the ferromagnetic nature of the experimental magnetic coupling constant is not unexpected as it is well known that $\mu_{1,1,1}$ -N₃ bridges transmit ferromagnetic interactions. Although no experimental magneto-structural correlation has been established yet for double ($\mu_{1,1}$ -N₃)-bridged dinuclear Ni^{II} complexes, however, as indicated elsewhere, DFT calculations²⁹ predict ferromagnetic interactions and a weak dependence on the Ni-N_{azide}-Ni angle (θ) so that J increases with θ to reach a maximum at $\sim 104^\circ$. The exchange coupling constants for **2** lies close to the lowest end of the range of values usually observed for this type of compound ($\sim +20$ cm⁻¹).^{25,28,31} It should be remarked that the structurally similar complex $[\text{NiNa}(\mu_{1,1,1}\text{-N}_3)(\mu\text{-}o\text{-vanillin})_2(\text{DMF})_2]$

exhibits a Ni-N_{azide}-N angle (100.63°) that are very close to that observed for the Na₂Ni₂ unit in **2** (101.33°) and, as expected, a magnetic coupling constant ($J = +20.2$) which is not far from the observed value for **2**.³² The slightly larger J_1 value observed for **2** compared to [NiNa($\mu_{1,1,1}$ -N₃)(μ -*o*-vanillin)₂(DMF)]₂ may be due, among other factors, to the bigger Ni-N_{azide}-N angle observed for the former complex and to differences in the coordination environments of the Ni^{II} ions in both compounds (NiN₄O₂ and NiN₂O₄). Nevertheless, the observed and calculated J_1 values for these compounds are significantly smaller than those found in other polynuclear Ni^{II} complexes with similar Ni-N-Ni angles but coplanar double $\mu_{1,1}$ -azide bridges connecting Ni^{II} ions, which could be due to the deviation of the $\mu_{1,1,1}$ -azide bridging ligand from the Ni-(N_{azide})₂-Ni plane, which as indicated the DFT calculations for the model compound of **1**, decrease the magnitude of the ferromagnetic interaction transmitted by the $\mu_{1,1}$ -azide bridging group. Anyway, we have performed DFT calculations on the model compounds [Ni₂(μ -EO)₂(NH₃)₈]²⁺, where the bridging fragment Ni(N_{azide})₂Ni and the $\mu_{1,1}$ -azide ligands are coplanar with a bridging angle $\theta = 100^\circ$ and Ni-N_{azide} distances of 2.1 Å. The τ angle (the shift of the $\mu_{1,1}$ -azide groups with regard to the Ni(N_{azide})₂Ni plane was varied between 0 and 30°. As can be observed in Figure S3, the deviation of the $\mu_{1,1}$ -azide group from the Ni-(N_{azide})₂-Ni plane provokes a slight but significant decrease of the ferromagnetic interactions. These theoretical results justify the relatively small J value for the interaction transmitted through the double $\mu_{1,1}$ -N₃ bridge in **2**.

Although there are some examples of polynuclear Ni₆ complexes containing the defective-dicubane Ni₄ unit observed in **3**,³³ to the best of our knowledge, this complex is the first genuine Ni₄ example with such a structure. The defective-cubane core of **3** exhibits three distinct magnetic exchange pathways between the Ni^{II} ions: (i) double $\mu_{1,1,1}$ -azide (ii) double $\mu_{1,1}$ -azide/ $\mu_{1,1,1}$ -azide and (iii) μ -phenoxido/ $\mu_{1,1,1}$ -azide, which are described by the coupling constant J_1 , J_3 and J_2 , respectively. As in the case of **2**, the ferromagnetic interactions found for **3** through (i) and (ii) exchange pathways are relatively small, due to the deviation of the $\mu_{1,1}$ -azide bridging ligand from the Ni-(N_{azide})₂-Ni plane, particularly in the case $\mu_{1,1}$ -azide groups. The fact that the pathway (i), bearing two $\mu_{1,1,1}$ -azide bridging groups (which show the larger deviation from the Ni-(N_{azide})₂-Ni plane), transmits a weaker ferromagnetic interaction than the pathway (ii), which contains only a $\mu_{1,1,1}$ -azide bridging group, is therefore not surprising. Regarding (iii), as far as we know, only five dinuclear complexes containing a mixed phenoxido/ $\mu_{1,1}$ -azide pathway have been reported so far,³⁴ which exhibit ferromagnetic interactions with J values between +5.7 and +51.2 cm⁻¹. Recent

2014/07/15

DFT theoretical studies^{34d} have predicted that the ferromagnetic exchange interaction mainly depends on the values of the corresponding Ni-O_{phenoxido}-Ni/Ni-O_{phenoxido} and Ni-N_{azide}-N/Ni-N_{azide} ratios as well as on the asymmetry of the two Ni-N_{azide} distances. Thus, the ferromagnetic interaction increases with increasing the Ni-N_{azide}-N/Ni-N_{azide} ratio and the asymmetry of the two Ni-N_{azide} distances, and decreases with decreasing the Ni-O_{phenoxido}-Ni/Ni-O_{phenoxido} ratio. Therefore phenoxido and $\mu_{1,1}$ -azide bridges have countercomplementary effects on the magnetic exchange coupling. Compound **3** has the phenoxido/ $\mu_{1,1,1}$ -azide bridging fragment with the lowest Ni-N_{azide}-Ni angle (92.88°), the longest Ni-N_{azide} distance and the largest deviation of the $\mu_{1,1,1}$ -azide ligand from the Ni-N_{azide}-Ni plane and therefore a very weak ferromagnetic interaction is expected, which agrees well with the experimental results.

The tetranuclear Ni₄ complex **4** has two different magnetic exchange pathways between Ni^{II} ions: (i) a mixed triple bridge μ -phenoxido/*syn-syn* acetate/ $\mu_{1,1}$ -azide and (ii) coplanar double $\mu_{1,1}$ -azide, which are described by the magnetic exchange parameters J_1 and J_2 , respectively. It should be noted that **4** is only the second example of a structurally and magnetically characterized Ni^{II} polynuclear complex where the mixed triple bridge μ -phenoxido/*syn-syn* acetate/ $\mu_{1,1}$ -azide is present. The first example is the trinuclear bent complex [Ni₃L³₂(OAc)₂($\mu_{1,1}$ -N₃)₂(H₂O)₂] (L³ = 2-[(3-dimethylaminopropylimino)-methyl]-phenol)³⁰ that exhibits a ferromagnetic exchange coupling through this mixed triple bridge with $J = +16.51 \text{ cm}^{-1}$. However, this magnetic coupling is significantly weaker than that found in **4** ($J_1 = +28.8 \text{ cm}^{-1}$), which may be due the fact that the Ni-O_{phenoxido}-Ni angle of 95.53° in **4** is expected to transmit ferromagnetic coupling whereas the same bridge in [Ni₃L³₂(OAc)₂($\mu_{1,1}$ -N₃)₂(H₂O)₂] with a Ni-O_{phenoxido}-Ni angle of 99.50° is expected to transmit antiferromagnetic coupling. Therefore, in **4** both phenoxido and $\mu_{1,1}$ -azide transmit ferromagnetic coupling whereas in [Ni₃L³₂(OAc)₂($\mu_{1,1}$ -N₃)₂(H₂O)₂] only the latter, which would lead to a stronger ferromagnetic coupling for the former. Although it is well known that the *syn-syn* acetate bridge transmits antiferromagnetic coupling, however when other bridges are present, as in the case of **4**, ferromagnetic coupling can be observed through countercomplementarity.³⁵ In fact, DFT calculations on diphenoxido-acetate compounds,²⁶ where the *syn-syn* acetate group has been substituted by two molecules of water, clearly show that the *syn-syn* acetate bridge has a ferromagnetic contribution to the exchange through countercomplementarity of $\sim +10 \text{ cm}^{-1}$.

As expected, the coplanar double $\mu_{1,1}$ -azide bridge mediated a strong ferromagnetic coupling ($J_2 = +81.9 \text{ cm}^{-1}$). As far as we know this is the larger ferromagnetic interaction ever observed transmitted by this type of bridge between Ni^{II} ions. Nevertheless, the strong ferromagnetic interaction mediated by the $\mu_{1,1}$ -azide bridge in **4** cannot be justified only by the magnitude of the Ni-N_{azide}-Ni bridging angle as compounds having similar bridging angles exhibit much lower J values, and there must be also consequence of the other ligands coordinated to the Ni^{II} ions. In fact, the influence of the non-bridging ligands on the magnitude of J has been extensively demonstrated in the literature.³⁶

It is worth mentioning that dynamic *ac* magnetic susceptibility measurements as a function of the temperature at different frequencies reveal that neither **3** nor **4** with $S = 4$ ground state exhibit slow relaxation of the magnetization and therefore SMM behaviour even in the presence of a small external *dc* field of 1000 G to fully or partly suppress the possible quantum tunneling relaxation of the magnetization.

Complex **5** has two different types of exchange pathways between the Ni^{II} ions: chlorophenoxido (described by J_1 and J_2) and di- μ_3 -chloro (described by J_3). Let us start with the di- μ_3 -chloro exchange pathway. Although a number of structurally and magnetically dichloro-bridged Ni^{II} complexes have been reported so far,³⁷ no clear magneto-structural correlation have been established yet. Nevertheless, experimental magneto-structural data for such a type of Ni^{II} complexes indicate that five-coordinated Ni^{II} ions usually exhibit antiferromagnetic interactions whereas octahedral or pseudooctahedral six coordinated Ni^{II} ions show ferromagnetic interactions with J values between $+5 \text{ cm}^{-1}$ and $+15 \text{ cm}^{-1}$. If the Ni^{II} ions are seriously tetragonally distorted the coupling could be antiferromagnetic. Moreover, the recently reported symmetrical cubane, $[\text{Ni}(\mu_3\text{-Cl})\text{Cl}(\text{HL}^4)]_4$ ($\text{HL}^4 = 2\text{-methyl-1-(pyridine-2-yl)propane-2-ol}$)³⁸ only containing di- μ_3 -chloro exchange pathways between the Ni^{II} ions exhibit a ferromagnetic exchange coupling with $J = +11.5 \text{ cm}^{-1}$. In complex **5** the Ni^{II} ions connected di- μ_3 -chloro bridges exhibit a distorted octahedral geometry and, therefore, a ferromagnetic interaction should be expected for this exchange pathway, which, together with the theoretical results, support the experimental set of J values where J_3 is ferromagnetic.

As for the phenoxido/chloro pathways described by J_1 and J_2 , the medium to strong antiferromagnetic interaction expected for the phenoxido exchange pathway with Ni-O-Ni angles of $\sim 114^\circ$ should be counterbalanced, at least partly, by the weak ferromagnetic interaction expected for the single-chloro exchange pathway. For instance, this

2014/07/15

counterbalance effect has been observed in a previously reported phenoxido/chloro dinuclear Ni^{II} complex,^{35c,39} with Ni-O-Ni and Ni-Cl-Ni angles of 105° and 85.35°, respectively, and a magnetic coupling $J = -1.17 \text{ cm}^{-1}$, whereas in the second one, with Ni-O-Ni and Ni-Cl-Ni angles of 103.6° and 83.78°, respectively, the magnetic coupling parameter was $J = +5.0 \text{ cm}^{-1}$. In this latter case, the decrease of the Ni-O-Ni reduce the antiferromagnetic exchange through the phenoxido bridge in some an extent that the ferromagnetic exchange through the Ni-Cl-Ni becomes predominant. In the case of **5**, with a larger Ni-O-Ni angle (~114°), a stronger antiferromagnetic interaction is expected for the magnetic coupling mediated by the phenoxido/chloro pathways, which agrees well with the theoretical J values.

Finally, Ni^{II} complexes containing only single-phenoxido bridges between the metal ions are rare,⁴⁰ exhibit Ni-O-Ni angles larger than 100° and consequently AF interactions between the Ni^{II} ions. To the best of our knowledge, compound **6** is the first example reported to date of a Ni₃ system with only such a type of bridge. Therefore, the AF interaction observed for **6** through the single-phenoxido exchange pathway with a Ni-O-Ni angle of ~119° is not surprising.

Conclusions

The flexible and versatile polytopic ligand *N,N'*-dimethyl-*N,N'*-bis(2-hydroxy-3-methoxy-5-methylbenzyl)ethylenediamine allows the preparation of six new polynuclear Ni^{II} complexes with uncommon/unique structures, ranging from Ni₂ to Ni₄, in which the ligand adopts a variety of bridging coordination modes. The formation of a specific complex depends on the satisfactory choice of both anion coligad and reaction conditions (metal to ligand molar ratio and solvent). Ni₂ complexes exhibit either double $\mu_{1,1,1}$ -azide bridge or rare di- μ -phenoxido/ $\mu_{1,1}$ -azide triple mixed bridges, which transmit medium and strong ferromagnetic interactions between the Ni^{II} ions, respectively, leading to a $S = 2$ ground state. Ni₄ azide containing complexes exhibit unique structures with bent and defective dicubane like topologies, depending on whether or not *syn-syn* acetate is additionally present in the structure. The complex with linear topology exhibits rare μ -phenoxido/ $\mu_{1,1}$ -azide/*syn-syn* acetate triple mixed bridges between central and terminal Ni^{II} atoms and a double $\mu_{1,1,1}$ -azide planar bridge between the central Ni^{II} ions, which communicate medium and very strong ferromagnetic interactions, respectively. The complex with defective-cubane Ni₄ core has two distinct types of mixed bridges, μ -phenoxido / $\mu_{1,1,1}$ -azido and $\mu_{1,1}$ -azido / $\mu_{1,1,1}$ -azido and a double di- $\mu_{1,1,1}$ -azido bridge, which mediate weak to medium ferromagnetic interactions between the Ni^{II} ions. Both Ni₄ azide containing complexes have an $S = 4$

ground state. The Ni₄ complex with chloride anions as coligands has a defective-dicubane structure with double μ -phenoxido/ μ_3 -chloro mixed bridges and di- μ_3 -chloro bridges, which propagate weak antiferro- and ferromagnetic interactions between the Ni^{II} ions, respectively, leading to a $S = 0$ ground state. Finally, Ni₃ complex with acetylacetonate as coligand exhibits a bent structure with very unusual single μ -phenoxido bridges and a weak antiferromagnetic interaction between the Ni^{II} leading to a $S = 1$ ground state. DFT calculations support the sign and magnitude of the experimental J values and help to correlate the structure and magnetic properties of these compounds. Although the Ni₄ azide containing complexes have an $S = 4$ ground state, none of them exhibit SMM behaviour.

Electronic Supplementary information (ESI)

X-ray crystallographic data for **1-6**, including data collection, refinement and selected bond lengths and angles, DFT calculations for the model compound [Ni₂(μ -_{1,1})₂(NH₃)₈]²⁺ and the M vs H plot for **6**.

Acknowledgements

Financial support from Ministerio de Economía y Competitividad (MINECO) for Project CTQ-2011-24478, the Junta de Andalucía (FQM-195 and the Project of excellence P11-FQM-7756), the University of Granada and Universidad del País Vasco are grateful acknowledged. We would like to thank the Centro de Supercomputación de la Universidad de Granada for computational resources. I. O. is grateful to the Departamento de Educación, Universidades e Investigación del Gobierno Vasco for a predoctoral fellowship. We are grateful to Nuria Clos, Unitat de Mesures Magnètiques Centers Científics i Tecnològics, Universitat de Barcelona, Spain. Technical and human support provided by SGIker (UPV/EHU, MINECO, GV/EJ, ERDF and ESF) for X-Ray measurements is gratefully acknowledged.

Notes and References

1 (a) *Concepts and Models in Bioinorganic Chemistry*, H. B. Kraatz and N. Metzler-Nolte (Ed), Wiley-VCH, Weinheim, Germany, 2006; (b) I. Bertini, H. B. Gray, E. I. Stiefeld, and J. S. Valentine, *Biological Inorganic Chemistry: Structure and Reactivity*, University

2014/07/15

- Science Books, 2007; (c) *Handbook of Metalloproteins*, A. Messerschmidt, R. Huber, T. Poulos and K. Wieghardt (Eds.), Wiley, Chichester, 2001; (d) *Nickel and its surprising impact in nature. Metal Ions in Life Sciences, vol.,2*; A. Sigel, H. Sigel and R. K. Sigel (Eds.), John Wiley and sons, Chichester, 2007; (e) J. L. Boer, S. B. Mulrooney and R. P. Hausinger, *Arch. Biochem. Biophys.* 2014, **544C**, 142 - 152 and references therein; (f) S. W. Ragsdale, *J. Biol. Chem.*, 2009, **284**, 18571–18575.
- 2 *Magnetism: Molecules to Materials, Vols. I–V*, J. S. Miller and M. Drillon, (Ed.), Wiley-VCH, Weinheim, Germany, 2001-2004.
- 3 (a) D. Gatteschi, R. Sessoli R. and J. Villain, *Molecular Nanomagnets*. Oxford University Press. Oxford, UK, 2006; (b) G. Aromí and E. K. Brechin, *Struct. Bond.*, 2006, **122**, 1–67; (c) J. N. Rebilly and T. Mallah; *Struct. Bond.*, 2006, **122**, 103–131; (d) A. Cornia, A. F. Costantino, L. Zobbi, A. Caneschi, D. Gatteschi, M. Mannini and R. Sessoli, *Struct. Bond.*, 2006, **122**, 133–161; (e) C. J. Milios, S. Piligkos and E. K. Brechin, *Dalton Trans.*, 2008, 1809-1817; (f) R. Bagai and G. Christou, *Chem. Soc. Rev.*, 2009, **38**, 1011-1026; (g) *Molecular Magnets, themed issue*, E. K. Brechin (Ed), *Dalton Trans.*, 2010; (f) *Molecular Cluster Magnets*. R. E. P. Winpenny (Ed.), World Scientific Books, Singapore 2011.
- 4 (a) A. R. Rocha, V. M. García-Suárez, S. W. Bailey, C. J. Lambert, J. Ferrerand, and S. Sanvito, *Nat. Mater.*, 2005, **4**, 335-339; (b) L. Bogani and W. Wernsdorfer, *Nat. Mater.*, 2008, **7**, 179-186; (c) M. Affronte, *Mater. Chem.*, 2009, **19**, 1731-1737; (d) M. N. Leuenberger and D. Loss, *Nature*, 2001, **410**, 789-793; (e) A. Ardavan, O. Rival, J. J. L. Morton, S. J. Blundell, A. M. Tyryshkin, G. A. Timco, G. A. and R. E. P. Winpenny, *Phys. Rev. Lett.*, 2007, **98**, 057201-057204. (f) P. C. E. Stamp and A. Gaita-Ariño, *J. Mater. Chem.*, 2009, **19**, 1718-1730.
- 5 *Molecular Magnetism*, O. Khan, VCH, Weinheim, Germany, **1993**.
- 6 L. Botana, J. Ruiz, J. M. Seco, A. J. Mota, A. Rodríguez-Diéguez, R. Sillanpää and E. Colacio, *Dalton Trans.*, 2011, **40**, 12462-12471.
- 7 Q. W. Xie, S. Q. Wu, C. M. Liu, A. L. Cui and H. Z. Kou, *Dalton Trans.*, 2013, **42**, 11227-12233.
- 8 (a) A. K. Boudalis, M. Pissas, C. P. Raptopoulou, V. Psycharis, B. Abarca and R. Ballesteros, *Inorg. Chem*, 2008, **47**, 10674-10681; (b) A. Ferguson, J. Lawrence, A. Parkin, J. Sanchez-Benitez, K. V. Kamenev, E. K. Brechin, W. Wernsdorfer, S. Hill, and M. Murrie, *Dalton Trans.*, 2008, 6409-6414; (c) A. Bell, G. Aromí, S. J. Teat, W. Wernsdorfer, and R. E. P. Winpenny, *Chem. Commun.*, 2005, 2808-2010. (d) D. I. Alexandropoulos, C. Papatriantafyllopoulou, G. Aromi, O. Roubeau, S. J. Teat, S. P.

- Perlepes, G. Christou and T. C. Stamatatos, *Inorg. Chem.* 2010, **49**, 3962-3964; (e) S. Petit, P. Neugebauer, G. Pilet, G. Chastanet, A. L. Barra, A. B. Antunes, W. Wernsdorfer, and D. Luneau, *Inorg. Chem.* 2012, **51**, 6645-6654 and references therein; (f) R. Biswas, Y. Ida, M. L. Baker, S. Biswas, P. Kar, H. Nojiri, T. Ishida, and A. Ghosh, *Chem. Eur. J.* 2013, **19**, 3943-3953; (g) H. Andres, R. Basler, A. J. Blake, C. Cadiou, G. Chaboussant, C. M. Grant, H. U. Güdel, M. Murrie, S. Parsons, C. Paulsen, F. Semadini, V. Villar, W. Wernsdorfer and R. E. P. Winpenny, *Chemistry*, 2002, **8**, 4867-4876; (h) R. T. W. Scott, L. F. Jones, I. Tidmarsh; S. B. Breeze, R. H. Laye, J. Wolowska, D. J. Stone, A. Collins, S. Parsons, W. Wernsdorfer, G. Aromi, E. J. L. McInnes and E. K. Brechin, *Chem. Eur. J.*, 2009, **15**, 12389-12398.
- 9 S. H. Kim, J. Lee, D. J. Kim, J. H. Moon, S. Yoon, H. J. Oh, Y. Do, Y. S. Ko, J. H. Yim and Y. Kim, *J. Organomet. Chem.* 2009, **694**, 3409-3417.
- 10 (a) A. D. Becke, *Phys. Rev. A*, 1988, **38**, 3098-3100; (b) C. T. Lee, W. T. Yang, and R. G. Parr, *Phys. Rev. B*, 1988, **37**, 785-789; (c) A. D. Becke, *J. Chem. Phys.*, 1993, **98**, 5648-5642.
- 11 M. J. Frisch, G. W. Trucks, H. B. Schlegel, G. E. Scuseria, M. A. Robb, J. R. Cheeseman, J. A. Montgomery Jr., T. Vreven, K. N. Kudin, J. C. Burant, J. M. Millam, S. S. Iyengar, J. Tomasi, V. Barone, B. Mennucci, M. Cossi, G. Scalmani, N. Rega, G. A. Petersson, H. Nakatsuji, M. Hada, M. Ehara, K. Toyota, R. Fukuda, J. Hasegawa, M. Ishida, T. Nakajima, Y. Honda, O. Kitao, H. Nakai, M. Klene, X. Li, J. E. Knox, H. P. Hratchian, J. B. Cross, C. Adamo, J. Jaramillo, R. Gomperts, R. E. Stratmann, O. Yazyev, A. J. Austin, R. Cammi, C. Pomelli, J. W. Ochterski, P. Y. Ayala, K. Morokuma, G. A. Voth, P. Salvador, J. J. Dannenberg, V. G. Zakrzewski, S. Dapprich, A. D. Daniels, M. C. Strain, O. Farkas, D. K. Malick, A. D. Rabuck, R. Raghavachari, J. B. Foresman, J. V. Ortiz, Q. Cui, A. G. Baboul, S. Clifford, J. Cioslowski, B. B. Stefanov, G. Liu, A. Liashenko, P. Piskorz, I. Komaromi, R. L. Martin, D. J. Fox, T. Keith, M. A. Al-Laham, C. Y. Peng, A. Nanayakkara, M. Challacombe, P. M. W. Gill, B. Johnson, W. Chen, M. W. Wong, C. Gonzalez and J. A. Pople, GAUSSIAN 03 (Revision C.0), Gaussian, Inc., Wallingford, CT, 2004.
- 12 G. B. Bacskay, *Chem. Phys.*, 1981, **61**, 385-404.
- 13 A. Schäfer, A.; C. Huber C and R. Ahlrichs, *J. Chem. Phys.*, 1994, **100**, 5829-5835.
- 14 Jaguar 7.6, Schrödinger, Inc., Portland, OR, 2009.

2014/07/15

- 15 (a) E. Ruiz, J. Cano, S. Alvarez, and P. Alemany, *J. Comput. Chem.*, 1999, **20**, 1391–1400; (b) E. Ruiz, S. Alvarez, A. Rodríguez-Forteza, P. Alemany, Y. Pucillon and C. Massobrio in *Magnetism: Molecules to Materials*, J. S. Miller and M. Drillon, (Eds.) Wiley-VCH, Weinheim, 2001, vol. II, p. 5572; (c) E. Ruiz, A. Rodríguez-Forteza, J. Cano, S. Alvarez and P. Alemany, *J. Comput. Chem.*, 2003, **24**, 982–989; (d) E. Ruiz, S. Alvarez, J. Cano and V. Polo, *J. Chem. Phys.*, 2005, **123**, 164110.
- 16 CrysAlisPro Software System; Agilent Technologies UK Ltd. Oxford, UK, 2012.
- 17 O. V. Dolomanov, L. J. Bourhis, R. J. Gildea, J. A. K. Howard and H. Puschmann, *J. Appl. Crystallogr.*, 2009, **42**, 339-341
- 18 G. M. Sheldrick, *Acta Crystallogr.*, 2008, **A64**, 112-122.
- 19 A. L. Spek, *Acta Crystallogr.*, 2009, **D65**, 148-155.
- 20 L. J. Farrugia, *J. Appl. Crystallogr.*, 1999, **32**, 837-838.
- 21 a) L. K. Das, A. Biswas, C. J. Gómez-García, M. G. B. Drew, A. Ghosh, *Inorg. Chem.* 2014, **53**, 434-445. b) P. Mukherjee, M. G. B. Drew, C. J. Gómez-García, A. Ghosh, *Inorg. Chem.* 2009, **48**, 4817-4827.
- 22 N. F. Chilton, R. P. Anderson, L. D. Turner, A. Soncini and K. S. Murray, *J. Comput. Chem.*, 2013, **34**, 1164-1175.
- 23 R. Boca, *Coord. Chem. Rev.*, 2004, **248**, 757-902.
- 24 A. J. Mota, A. Rodríguez-Diéguez, M. A. Palacios, J. M. Herrera, D. Luneau and E. Colacio, *Inorg. Chem.*, 2010, **49**, 8986-96.
- 25 P. Mukherjee, M. G.B. Drew, C. J. Gómez-García, and A. Ghosh, *Inorg. Chem.*, 2009, **48**, 5848-5860.
- 26 M. P. Palacios, A. J. Mota, J. E. Perea-Buceta, F. J. White, E. K. Brechin and E. Colacio, *Inorg. Chem.*, 2010, **49**, 10156-10165.
- 27 (a) R. Biswas, S. Giri, S. K. Saha and A. Ghosh, *Eur. J. Inorg. Chem.*, 2012, 2916–1927; (b) K. K. Nanda, L. K.; Thompson, J. N. Bridson and K. Nag, *J. Chem. Soc. Chem. Commun.*, 1994, 1337-1338; (c) M. A. Halcrow, J. S. Sun, J. C. Huffman and G. Christou, *Inorg. Chem.*, 1995, **34**, 4167-4177; (d) J. M. Clemente-Juan, B. Chansou, B. Donnadieu and J. P. Tuchagues, *Inorg. Chem.*, 2000, **39**, 5515-5519; (e) X. H. Bu, M. Du, L. Zhang, D. Z. Liao, J. K. Tang, R. H. Zhang and M. Shionoya, *J. Chem. Soc. Dalton Trans.*, 2001, 593- 598.

- 28 J. Ribas, A. Escuer, M. Montfort, R. Vicente, R. Cortes, L. Lezama, and T. Rojo, *Coord.Chem. Rev.*, 1999, **193–195**, 1027-1068.
- 29 E. Ruiz, J. Cano, S. Alvarez and P. Alemany, *J. Am. Chem. Soc.*, 1998, **120**, 11122-11129.
- 30 R. Biswas, S. Mukherjee, P. Kar, and A. Ghosh, *Inorg. Chem.*, 2012, **51**, 8150-8160.
- 31 A. Solanki, M. Monfort, S. B. Baran Kumar, *J. Mol. Struct.* 2013, **1050**, 197–203.
- 32 S. H. Zhang, N. Li, C. M. Ge, C. Feng and L. F. Ma, *Dalton Trans.*, 2011, **40**, 3000-3007.
- 33 a) A. Escuer, G. Aromí, *Eur. J. Inorg. Chem.* 2006, 472. b) S. Tandon, S. D. Bunge, R. Rakosi, Z. Xu, L. K. Thompson, *Dalton, Trans.* 2009, 6536. c) X.-T. Wang, B.-W. Wang, Z.-M. Wang, W. Zheng, S. Gao, *Inorg. Chim. Acta, Inorg. Chim. Acta*, 2008, **361**, 3895.
- 34 (a) R. Koner, S. Hazra, M. Fleck, A. Jana, C. R. Lucas and S. Mohanta, *Eur. J. Inorg. Chem.*, 2009, 4982-4988; (b) S. K. Dey, N. Mondal, M. S. E. Fallah, R. Vicente, A. Escuer, X. Solans, M. Font-Bardía, T. Matsushita, V. Gramlich and S. Mitra, *Inorg. Chem.*, 2004, **43**, 2427-2434; (c) A. Banerjee, R. Singh, D. Chopra, E. Colacio and K. K. Rajak, *Dalton Trans.*; 2008, 6539-6545; (d) S. Sasmal, S. Hazra, P. Kundu, S. Dutta, G. Rajaraman, E. Carolina Sañudo and S. Mohanta, *Inorg. Chem.*, 2011, **50**, 7257-7267.
- 35 (a) P. Mukherjee, M. G. B. Drew, V. Tangoulis, M. Estrader, C. Diaz and A. Ghosh, *Inorg. Chem. Commun.*, 2009, **12**, 929-932; (b) J. Ruiz, A. J. Mota, A. Rodríguez-Diéguez, I. Oyarzabal, J. M. Seco and E. Colacio, *Dalton Trans.*, 2012 **41**, 14265-142673.
- 36 P. Román, C. Guzmán-Miralles, A. Luque, J. I. Beitia, J. Cano, F. Lloret, M. Julve and S. Alvarez, *Inorg. Chem.*, 1996, **35**, 3741-3751.
- 37 (a) B. Tong, S. C. Chang, E. E. Carpenter, C. J. O'Connor, J. O. Lay Jr., J. O.; R. E. Norman, *Inorg. Chim. Acta*, 2000, **300–302**, 855–861; (b) G. A. van Albada, J. J. A. Kolnaara, W. J. J. Smeets, A. L. Spek, and J. Reedijk, *Eur. J. Inorg. Chem.*, 1998, 1337-1341; (c) E. Viñuelas-Zahinos, F. Luna-Giles, P. Torres-García and A. Bernalte-García, *Polyhedron*, 2009, **28**, 1362-1368.
- 38 S. Hameury, L. Kayser, R. Pattacini, G. Rogez, W. Wernsdorfer and P. Braunstein, *Dalton Trans.*, 2013, **42**, 5013-5024 .
- 39 E. R. Quijano, E. D. Stevens and C. J. O'Connor, *Inorg. Chim. Acta*, 1990, **177**, 267-275.
- 40 S. Mandal, V. Balamurugan, F. Lloret, and R. Mukherjee, *Inorg. Chem.*, 2009, **48**, 7544-7556.